Washington University in St. Louis
Washington University Open Scholarship

All Theses and Dissertations (ETDs)

Summer 8-19-2013

Microdevices for Isolating Single Axons for the Study of Axonal Transport in Dopaminergic Neurons

Xi Lu
Washington University in St. Louis

Follow this and additional works at: https://openscholarship.wustl.edu/etd

Recommended Citation
Lu, Xi, "Microdevices for Isolating Single Axons for the Study of Axonal Transport in Dopaminergic Neurons" (2013). *All Theses and Dissertations (ETDs)*. 1146.
https://openscholarship.wustl.edu/etd/1146

This Dissertation is brought to you for free and open access by Washington University Open Scholarship. It has been accepted for inclusion in All Theses and Dissertations (ETDs) by an authorized administrator of Washington University Open Scholarship. For more information, please contact digital@wumail.wustl.edu.

WASHINGTON UNIVERSITY IN ST. LOUIS

School of Engineering and Applied Sciences

Department of Biomedical Engineering

Dissertation Examination Committee:
Shelly Sakiyama-Elbert, Chair
Dennis Barbour
Paul Bridgman
Joshua Maurer
Karen O'Malley
Jin-Yu Shao

Microdevices for Isolating Single Axons for the Study of Axonal Transport in Dopaminergic Neurons

By

Xi Lu

A dissertation presented to the
Graduate School of Arts and Sciences
of Washington University
in partial fulfillment of the
requirements for the degree of

Doctor of Philosophy

August 2013
St. Louis, Missouri

Contents

List of Figures

List of Tables

Acknowledgements

I would like to thank my PhD advisor, Dr. Shelly Sakiyama-Elbert, for the chance to pursue my degree in her lab. Her support, guidance and patience have given me a great opportunity to grow as a scientist, communicator, and critical thinker. Thank you for everything.

I would like to thank all past and present members of the Sakiyama-Elbert lab with whom I have had the privilege of working and becoming friends with: Dr. Matt Wood, Dr. Phil Johnson, Dr. Nithya Jesuraj, Dr. Dylan Mcreedy, Dr. Amy Harkins, Dr. Emily Crownover, Rich Seeger, Hao Xu, Laura Marquardt, Thomas Wilems, Lin Bai, Nisha Iyer, Alexander Tatara, Jessica Butts, Chelsea Brown, and Jasmine Kwasa. I would also like to thank Sara Oswald for being so encouraging, doing a great job managing the lab and making our lives easier. I am grateful to you all for the support, fun times, and welcoming atmosphere that have made the lab a wonderful place to work.

I would like to thank everyone in Dr. Karen O'Malley's lab for adopting me as one of their own during my graduate school career. I would like to thank Dr. Karen O'Malley for the opportunity to work with her lab and learn from her expertise, Steve Harmon for tirelessly performing animal dissections and teaching me many scientific techniques, Dr. Ivy Jong for helping to troubleshoot my experiments, and other members of the lab, Dr. Jo Ann Antenor-Dorsey, Dr. Ismail Sergin, and Carolyn Purgert for helping to create a wonderfully friendly environment. Finally, I would like to express my deepest gratitude to Dr. Jeongsook-Kim Han for her invaluable help and support. Her generosity, kindness and scientific expertise have provided me guidance on not only being a better scientist but also a better person.

I am grateful for the assistance of many centers at Washington University in St. Louis. I would like to thank the Nanotechnology Research facility for helping with making the silicon masters. I would like to thank the Bakewell Imaging Center and in particular, Mr. Dennis Oakley for all things related with microscopy and imaging.

I would like to thank members of my committee, Dr. Dennis Barbour, Dr. Jin-Yu Shao, Dr. Paul Bridgman, and Dr. Joshua Maurer for their expertise and guidance in helping me complete my project. I would also like to thank my funding sources: The National Institutes of Health and Washington University in St. Louis.

I would also like to thank all of my friends from graduate and undergraduate school. While there is no space to list everyone, their love and belief in me have helped to carry me through graduate school and enriched my life in ways I would have never expected.

Finally, I would like to dedicate this thesis to my parents, Xian Lin and Yuan Lu, and thank them for helping me to become the person that I am today. Your love and unyielding strength are qualities to which I will always aspire. Knowing that there is always home provides not only comfort and security but also makes the unknown paths of life much more exciting.

Xi Lu

Washington University in St. Louis

August 2013

ABSTRACT OF THE DISSERTATION

Microdevice for Isolating Single Axons for the Study

of Axonal Transport in Dopaminergic Neurons

By

Xi Lu

Doctor of Philosophy in Biomedical Engineering

Washington University in St. Louis, 2013

Professor Shelly Sakiyama-Elbert, Chair.

Axonal degeneration plays an important role in the etiology of major central nervous system (CNS) neurodegenerative disorders such as Parkinson's disease (PD) but investigations into the mechanisms underlying this important process has been limited. The goal of this dissertation was to design and demonstrate the use of a compartmented microdevice which allows for the isolation and study of axonal processes such as mitochondrial transport away from cell neuronal bodies. To achieve this goal, a PDMS microdevice comprised of two large chambers connected by a parallel array of microchannels successfully achieved separation of axons from the soma and allows tracking of transport along oriented axons. To create an *in vitro* model of PD, dopaminergic axons from midbrain cultures were isolated within the microchannels away from the cell bodies. To determine the best method for imaging intracellular organelles, cells were transduced with a mitochondria targeted DsRed2 lentiviral vector or with a mitochondria specific dye, Mitotracker Deep Red. While both methods successfully labeled the mitochondria, the dye, created significant fluorescent background noise which made measuring mitochondria movement difficult. Using the microdevice, the effects of 6-hydroxydopamine (6-OHDA), one of the most commonly used toxins for modeling PD, on axonal transport was then investigated on GFP labeled midbrain neurons cultured within the microdevice. 6-OHDA quickly induced mitochondrial transport dysfunction in both GFP and

non-GFP labeled axons. Transport of synaptic vesicles were also blocked by the effects of 6-OHDA. 6-OHDA also induced the fragmentation of microtubules and the induction of autophagy but these processes came at a much later time point compared to transport inhibition. These toxin effects on mitochondrial transport were blocked by the addition of SOD1-mimetic, Mn(III)tetrakis(4-benzoic acid)porphyrin chloride (MnTBAP), as well as the anti-oxidant N-acetyl-cysteine (NAC). However, addition of calcium ion chelator, ethylene glycol tetraacetic acid (EGTA), did not restore mitochondrial transport. This study suggests that transport dysfunction occur early and may play a significant role in inducing axonal degeneration in response to 6-OHDA treatment. Overall, the dissertation shows that the microdevice is an excellent tool for studying axonal degenerative processes in the CNS.

Chapter 1

Introduction

1.1 Overview

This work describes the design and use of a compartmented microdevice that allows for the isolation and study of axons apart from the cell body and dendrites. The motivation behind the work is the important initial role that axonal degeneration plays in the onset and progression of major neurodegenerative diseases, such as Parkinson's disease (PD), Alzheimer's disease and Huntington's disease. When designing therapies, it is important to understand and target the molecular pathways involved in the earlier stages of the degenerative process rather than targeting more downstream events. Many therapies that have been designed to rescue cell bodies in neurodegenerative diseases show little efficacy in slowing disease progression. This may be due to axonal degeneration being the initial locus of disease. Unfortunately, designing treatments to preserve axonal structure and function remains an incredible challenge simply because of the limited knowledge available regarding the pathways that underlie the axonal degeneration process. One of the main obstacles is the limited availability of tools to study the degenerative process within the axons of central nervous system (CNS) neurons. Technical challenges that must be overcome in order to obtain more accurate PD models include maintaining viability of the oft-times fragile primary CNS neuronal cultures *in vitro*, stimulating axonal outgrowth, and isolating axons so that they may be studied without confounding effects from the cell body or dendrites .

One of the key conundrums of PD is the apparent specific vulnerability of dopaminergic (DA) neurons to degeneration, at least in the earlier phases of the disease, and it is not clear what properties make them so vulnerable in PD. The fragility and scarcity of DA neurons within the

midbrain (5-10% of the entire midbrain neuronal population) is an important consideration. Regardless, in order to properly understand the disease pathology, it is important to study actual midbrain DA neurons and axons rather than a cell line or neurons of other lineage.

The first aim was to create a microdevice using soft lithographic techniques that allowed for culture and separation of midbrain DA neurons from their axons within fluidically-isolated chambers. Murine mesencephalic cultures were obtained and cultured within the microdevices for up to 30 days to show that long-term culture could be maintained. On average, it took approximately 8-10 days for axons to fully cross between compartments. To optimize single axon visualization, the extent of neurite penetration and axonal bundling were assessed for various geometric parameters. As well as culture and assay conditions. As axons extend, they may naturally bundle with one another with one leading axon serving as a guide for others. To avoid any activation of secondary pathways from biochemical bundling inhibition, physical aspects of the microchannels were redesigned to optimize finding and imaging single oriented axons. In addition to isolating the axons, the material properties of the elastomer used to create the microfluidic device was considered to identify the best techniques for visualizing intra-axonal organelle movement. It was found that the adsorbent nature of the microdevice material was not conducive to fluorescent dye visualization of mitochondrial movement. Therefore, a lentiviral vector for an organelle-specific fluorescent protein was used to visualize mitochondria and other vesicles during live-cell imaging.

The final study was done to investigate the effects of 6-hydroxydopamine (6-OHDA) on axonal transport within midbrain cultures. Disruption to the movement of organelles and vesicles is commonly observed within axonopathies and occurs early within the degenerative process. 6-OHDA is a commonly used toxin to induce parkinsonism and is a model of an acute form of PD. While it does not completely recapitulate all of the symptoms of sporadic PD, it is frequently used to

establish the efficacy of potential PD therapeutics as it reliably produces axonal degeneration of DA neurons in the nigrostriatal pathway *in vivo*. The microdevices were used to explore how 6-OHDA affects various aspects of axonal transport, such as mitochondria and synaptic vesicle movement in anterograde and retrograde directions, integrity of tracks for transport, and potential underlying mechanisms, which may explain how 6-OHDA exerts its toxicity. Using 6-OHDA and the microdevice, I was able to establish that disruption to axonal transport of mitochondria and synaptic vesicles transport was an early event in the onset of axonal degeneration. These transport disruptions may be due to excess ROS produced by 6-OHDA.

This chapter will provide a general introduction to PD, which includes current theories and models regarding the mechanisms that underlie the neurodegenerative process in PD. This chapter will also cover some of available methodologies to study specific segments of the neuron, such as axons and dendrites, and the limitations to those methods. Additionally, new soft lithographic techniques such as microfabrication will be explored to developing tools for studying neurodegenerative diseases.

1.2 Parkinson's Disease

1.2.1 An Overview of Parkinson's Disease

Parkinsonism has been known since ancient times but was not medically described until 1817 by Dr. James Parkinson in his work "An Essay on the Shaking Palsy"(Parkinson 1817). Additional important and more thorough investigations of the malady came later from the works of investigators, such as Jean Martin-Charcot, to fully establish the clinical spectrum of Parkinson's disease (PD) (Charcot and Bourneville 1872). Since then, PD has been established as second most

common neurodegenerative disease in the United States and the most common moto-degenerative disease. It is estimated that there are currently 1 million PD patients in the United States and more than 5 million sufferers around the world (Olanow, Stern et al. 2009). Arguably, the greatest risk factor for PD is old age, as the chances of getting PD increases dramatically over the age of 60 (Driver, Logroscino et al. 2009). However, certain forms of familial PD show symptoms earlier in life: between late 30s and early 40s (Schrag and Schott 2006). The cardinal motor hallmarks of PD are: bradykinesia or slowness of movement, rigidity, resting tremors and postural instability (Lees, Hardy et al. 2009). These motor symptoms are associated with the death of dopaminergic (DA) neurons that are part of the nigrostriatal pathways. The cell bodies of these DA neurons lie within the Substantia Nigra par compacta (SNpc) and extend their axons into areas of the striatum, such as the caudate and putamen (Dauer and Przedborski 2003). After centuries of investigation, the mechanisms responsible for the death of these neurons remain elusive. It has been estimated that 85% of all PD cases are classified as sporadic in which there is no known cause, and 15% of the cases are familial with both autosomal dominant and recessive mutations contributing to the onset of PD symptoms (Corti, Lesage et al. 2011). Pathological features of PD include eosinophilic aggregates of misfolded proteins known as Lewy bodies and Lewy neurites. The major protein identified within these aggregates is α-synuclein, but other proteins are also found within the Lewy bodies, such as tau and ubiquitin (Spillantini, Schmidt et al. 1997). Lewy bodies are also found within peripheral systems (Wakabayashi, Takahashi et al. 1988). Whether these misfolded protein aggregates are a causative factor in PD and contribute to the progression of the disease, or are simply symptoms of breakdowns in the protein clearance systems, remain unclear.

Advances in understanding of PD remained stagnant until the discovery of dopamine and its localization within the striatum in the mid-twentieth century. An accompanying major discovery was that levodopa, a natural precursor to dopamine, reversed the effects of parkinsonism in toxin

models and eventually PD in patients. However, without a clear understanding of the mechanism underlying the disease process, it has been impossible to establish a cure or treatment to delay the disease's progression. Currently, Levodopa remains the gold standard of treatment for PD, but eventually its efficacy wanes and there is the development of unwanted side effects, such as dyskinesia or uncontrolled movement of the body. Mood disorders are also associated with heavy levodopa use, such as agitation, confusion, anxiety, and hallucination (Olanow, Agid et al. 2004). Most other medications for PD are designed around the idea of making dopamine more available whether it is through limiting the degradation of dopamine/levodopa, acting as agonists of dopamine receptors, or being stabilizers to ensure a steady and constant supply of levodopa. Other treatments, such as deep brain stimulation, have shown efficacy in reducing the motor symptoms of PD, but the mechanism of these treatments remains unknown (Rodriguez-Oroz, Obeso et al. 2005; Nilsson, Patel et al. 2013).

While PD has been classically described as a motor disorder, it is clear now that many other non-motor symptoms exist. Autonomic dysfunctions, cognitive deficits, such as memory loss and confusion, disturbances to sleep and other behavioral disorders are also common to PD sufferers. Degeneration of hippocampal and cholinergic structures have been observed with the deaths of cholinergic (Candy, Perry et al. 1983), noradrenergic (Greenfield and Bosanquet 1953), and serotonergic neurons (Scatton, Dennis et al. 1986). Adding to the confusion is the uncertainty that the motor deficits seen in PD are part of the early phases of the disease. It has also been suggested that the disease may actually begin elsewhere in the brain and even that PD is not a single disorder with a singular cause (Cheng, Ulane et al. 2010). Part of the difficulty in establishing a clear definition of PD and developing a cure is the lack of a good animal model that recapitulates all of the features seen in PD.

1.2.2 Genetic Models of PD

The growing list of gene mutations (particularly within the Park family) that contribute to familial PD has made genetics an important piece in understanding in the complex etiology of PD. Autosomal dominant forms of hereditary PD include mutations to SNCA (Polymeropoulos, Lavedan et al. 1997), one of the first PD genes to be sequenced, that codes for α-synuclein, and leucine-rich repeat kinase 2 (LRRK2) (Zimprich, Biskup et al. 2004). In addition to point mutations of SNCA gene, overexpression of SNCA have led to a PD pathology (Singleton, Farrer et al. 2003). Unfortunately, the endogenous function of α-synuclein is unknown despite being enriched at the axon terminal (Maroteaux, Campanelli et al. 1988) and involved with vesicles trafficking and storage of neurotransmitters (Kramer and Schulz-Schaeffer 2007). How SNCA interacts with other protein targets of PD mutations is still unclear. Common recessive forms of familial of PD include Pink1 (Rohe, Montagna et al. 2004), DJ-1 (Bonifati, Rizzu et al. 2003), and Parkin (Kitada, Asakawa et al. 1998). Investigation into the targets of PD mutants have made important contributions to the understanding of many biological processes (Shulman, De Jager et al. 2011).

A common thread in many of the familial forms of PD is the link to mitochondrial regulation. Pink1 and Parkin have been linked to a common pathway (Narendra, Jin et al. 2010) that regulates key aspects of mitochondria dynamics, such as mitochondria quality control (Narendra, Walker et al. 2012), calcium homeostasis (Heeman, Van den Haute et al. 2011), fission (Liu, Acin-Perez et al. 2011) and fusion (Poole, Thomas et al. 2010; Liu, Acin-Perez et al. 2011) , as well as regulation of mitochondrial transport (Wang, Winter et al. 2011). These regulatory factors, which are localized to the mitochondrial membrane, have contributed greatly to uncover mechanisms that may potentially explain why mitochondria are vulnerable in many different forms of PD. In

addition to the mitochondria, Parkin has also been shown to play roles in ubiquitin-proteasome systems (Tanaka, Cleland et al. 2010).

Despite the mechanistic insight into mitochondrial regulation gained from studies with Pink1 and Parkin, there are still many caveats to using these genetic models of PD. Knockdown of PD genes, such as Pink1 and Parkin in Drosophila using RNAi have beautifully recreated the loss of DA neurons seen in sporadic PD with the associated motor defects (Wang, Qian et al. 2006; Yang, Gehrke et al. 2006), However, double and triple knockouts of Pink1, Parkin and DJ-1 in mice have led to very mild motor symptoms and no progressive loss of DA neurons (Goldberg, Fleming et al. 2003; Palacino, Sagi et al. 2004; Gispert, Ricciardi et al. 2009; Kitada, Tong et al. 2009). These *in vivo* results suggest the presence of compensatory mechanisms in place to maintain neuronal function. Regardless, PD toxin models remain the gold standard for developing and testing therapeutics for PD, as well as understanding the mechanisms for degeneration of DA neurons.

1.2.3 Environmental Models of PD

1.2.3.1 MPP+

Currently, the gold standard for modeling toxin-induced degeneration of DA neurons is 1-methyl-4-phenyl-4-propionoxypiperidine or MPTP. Its crosses the blood brain barrier where it is taken up by astrocytes and converted into its active metabolite MPP+ by monoamine oxidase B (MAO-B) (Markey, Johannessen et al. 1984). MPP+ is then released into the extracellular milieu and taken up by DA neurons via the dopamine transporter (DAT). MPP+ has also shown slight affinity for other catecholaminergic transporters.

MPTP was created in the early 1980s from street user's attempt to synthesize the narcotic meperidine (Davis, Williams et al. 1979). To the surprise of doctors and researchers, the users quickly developed irreversible and severe parkinsonian symptoms (Langston, Ballard et al. 1983). Administration of MPTP in monkeys show similar patterns of striatal DA degeneration and cell loss within the SNpc. Both primates and humans affected by MPP+ have responded well to treatments with levodopa (Langston, Ballard et al. 1983). Despite being mostly selective for DA neurons, not all features of sporadic PD are present in the MPP+ model of cell degeneration as there is inconsistent loss of monaminergic neurons within the locus coeruleus (Forno, Langston et al. 1986) and also lack of Lewy body formation (Davis, Williams et al. 1979; Forno, DeLanney et al. 1993).

Once inside the cell, MPP+ has been shown to be sequestered inside the mitochondria where subsequently there is disruption to the activities of the electron transport chain via Complex I. This disruption may then lead to mitochondrial damage and energy loss within the cell (Ramsay and Singer 1986; Surmeier, Guzman et al. 2010). MPP+ has also been shown to be a substrate for vesicular monoamine transporter 2 (VMAT2), and MPP+ has been hypothesized to induce the release of the highly reactive dopamine from its intracellular stores (Lotharius and O'Malley 2000; Staal and Sonsalla 2000). The mechanism for MPP+ induced cellular degeneration does not completely resemble necrosis or apoptosis (Choi, Canzoniero et al. 1999; O'Malley, Liu et al. 2003). The observation that genetic models of PD and MPP+ both affect mitochondrial processes presented an exciting link between sporadic and familial forms of the disease. So far, it has been unclear whether environmental factors (such as pesticides, toxins or heavy metals) or genetic factors (or both) play significant part in the onset of PD. It may also turn out that multiple causes may lead to PD and other parkinsonisms, but if they converge on a single or a few target pathways then those

pathways would be the more realistic and ideal targets for the development of therapies (Burke and O'Malley 2012).

1.2.3.2 6-hydroxydopamine (6-OHDA)

Discovered in the 1950s, 6-hydroxydopamine or 6-OHDA was the first toxin to lesion the nigrostriatal DA pathway, and is frequently used to generate behavioral and physiological effects *in vivo,* as well as to screen for therapies that may improve PD symptoms (Ungerstedt 1968). 6-OHDA is a naturally occurring and highly reactive hydroxylated analog of dopamine (Curtius, Wolfensberger et al. 1974) and does not cross the blood brain barrier. It has shown a high affinity for catecholaminergic transporters, such as DAT and norepinephrine transporters as catecholaminergic blockers have blocked 6-OHDA toxicity *in vivo*(Breese and Traylor 1970). To produce more specificity *in vivo*, it is often injected in conjunction with a noradrenaline reuptake inhibitor, such as desipramine (Luthman, Fredriksson et al. 1989).

In vivo, 6-OHDA is directly injected into areas of the striatum or substantia nigra in order to produce retrograde or anterograde, respectively, models of DA degeneration. While its degenerative effects are highly reproducible, the toxin does not mimic all of the effects of PD, such as cell death in other brain regions, such as olfactory bulb and brain stem. Also missing are signs of Lewy-like inclusions seen in PD (Schober 2004).

In addition to being transported into the cell via DAT in *in vitro* models, 6-OHDA has been shown to inhibit mitochondrial complex I and IV (Glinka and Youdim 1995) as well as oxidizing readily to generate reactive oxygen species, such as hydrogen peroxide (Saito, Nishio et al. 2007) as well as p-quinones (Monteiro and Winterbourn 1989) extracellularly thus leading to higher levels of

oxidative stress (Holtz, Turetzky et al. 2005; Holtz, Turetzky et al. 2006). Therefore, the exact pathway by which 6-OHDA exerts its toxic effects is highly controversial. Studies using cell lines with and without DAT have yielded variable results of intra vs. extracellular 6-OHDA mechanisms (Clement, Long et al. 2002; Hanrott, Gudmunsen et al. 2006; Redman, Jefferson et al. 2006). Whatever the route, 6-OHDA has been shown to inhibit complex I and induce collapse in mitochondrial membrane potential (Lotharius, Dugan et al. 1999) and p53 activation (Bernstein, Garrison et al. 2011). 6-OHDA has also been shown to induce an apoptotic version of cell death (Choi, Yoon et al. 1999; Marti, Saura et al. 2002) with observations of increased DNA fragmentation, cytochrome c release, and caspase activation (Holtz and O'Malley 2003).

While patient studies and experimental data have revealed an incredible amount of data on where PD degeneration occurs at the level of large structures within the brain, the actual cellular processes remain a mystery. Despite knowing that MPP+ is sequestered inside of mitochondria and 6-OHDA may activate apoptotic pathways, the actual chain of events which lead to these effects isn't clear. In fact, a significant research effort has been underway to determine where the degeneration initiates.

1.3 Mechanisms of PD

1.3.1 Axonal Degeneration in PD

Unlike many other somatic cells, the neuron has a highly compartmentalized structure. The simplest model of a neuron can be conceptualized as three distinct compartments: dendrites, the cell body (somal), and the axon. The dendrites and the cell body receive and process inputs that can then be used to generate an output, such as neurotransmitter release via the axon. Without a viable

axon or synaptic terminal, neurons would lose the means to perform their function and carry signals to the target. In addition to being sites of neurotransmitter release, the synapses are also the sites where neurotransmitters are produced and where growth factors may be taken up and transported in a retrograde fashion towards the cell body where they act as survival signals.

The more significant depletion of DA signals within the striatum compared to the SNpc suggests that the cell body may not actually be the initial site of injury but that degeneration could initiate along the axon. If this were true, then treatments that target the maintenance of axonal functionality and integrity could potentially have greater efficacy in overcoming degenerative diseases. It is of interest to note that axon degeneration is a phenomenon that is seen not only in PD but also in other major neurodegenerative diseases, such as Alzheimer's and Huntington's disease (Coleman 2005). Therefore, understanding the process of axonal degeneration in PD could potentially provide clues to understanding cell death in other diseases as well. The following sections will cover patient and experimental data which suggests the existence and importance of axonal degeneration.

1.3.2 Patient and Functional Imaging Data in PD

Patient data from post-mortem studies showed a distinct dopaminergic deficiency in PD patients. Since dopamine is primarily synthesized at the axonal terminal and dopamine transporters are enriched within the striatum (Ehringer and Hornykiewicz 1960), it was proposed by Dr. Oleh Hornykiewicz that degeneration at the cellular level first begin at the axons and proceeds towards the Substantia Nigral cell bodies in a "dying back" fashion (Hornykiewicz 1998). Regression analysis of cell count versus PD duration found that at the onset of motor symptoms, there is a 31% loss of

the cell bodies with signs of incidental Lewy bodies (Fearnley and Lees 1991). Concurrently, there has been a much more substantial loss of DA terminals within the striatum (Bernheimer, Birkmayer et al. 1973). Post mortem measurement of dopamine levels in the caudate show that at the onset of motor symptoms there is a 68-82% loss of striatal DA signal (Riederer and Wuketich 1976). Functional imaging PET studies have supported the previous findings that striatal DA terminal loss occurs significantly before death of the cell bodies (Lee, Samii et al. 2000). Using radioligand imaging analysis of striatal DA markers, such as levodopa metabolism, dopamine transporter, or vesicular monoamine transporter (responsible for sequestering dopamine within vesicles), it was found that at the onset of motor symptoms, there was a 50-70% loss of ligand labeling at the onset of motor symptoms in PD (Nandhagopal, McKeown et al. 2008).

1.3.3 Toxin and Genetic Models of Axonal Degeneration in PD

The protein aggregates known as Lewy bodies are a distinct pathological hallmark of PD and it is of interest to note that Lewy neurites form prior to Lewy bodies. Studies that looked at the development of α-synuclein pathology have found that the degenerative process typically begins within the axon and may proceed retrogradely (Orimo, Uchihara et al. 2008) showing distinct loss of dopamine release, striatal dopaminergic pathology, and reduction of synaptic and motor proteins (Chu, Morfini et al. 2012) prior to the significant loss of DA cell bodies. In addition to α-synuclein, mice with LRRK2 mutations showed preservation of DA cell bodies but significant loss of striatal tyrosine hydroxylase (TH) immunoreactivity (Li, Liu et al. 2009). Tyrosine hydroxylase is the rate limiting enzyme for production of dopamine and is often used as a marker for identifying DA neurons. While Parkin knockout mouse models have not exhibited the same degree of DA pathology as the autosomal dominant models of PD (Palacino, Sagi et al. 2004), Perkin's role in

supporting mitochondrial health and transport suggests that maintenance of axon function and health is important.

Results from PD toxin models continue to support the idea that axons are a major target for degeneration and disruption. In primate models of MPP+, the pattern of degeneration recapitulates what has been seen in humans, where severe degradation of the terminal fields occur prior to serious loss of cell bodies within the substantia nigra (Herkenham, Little et al. 1991). Chronic application of MPP+ in mice showed a similar pattern with 80% loss of DAT staining and only 43% decline in SNPc cell bodies (Meissner, Prunier et al. 2003). Additionally, in rodent models, injection of 6-OHDA into the striatum led to depletion of dopamine rapidly and induced a progressive retrograde degeneration (Blum, Torch et al. 2001). Unfortunately, it is not known just how exactly the toxins and genetic models cause axonal degeneration. However, one common feature of axonal degeneration in PD and in other degenerative diseases is a disruption to axonal transport

1.4 Axonal Transport

Axons vary diversely in both length and size with some motor axons being over 1 m in length. As the protein translation machinery present within the axon is quite limited, transport of proteins is required for maintaining axonal structures, such as receptors, ion channels, and cytoskeletal molecules. Delivery of synaptic vesicles, growth factors, and power generating organelles such as the mitochondria also occurs via axonal transport machinery. Cytoskeletal structures, such as microtubules and neurofilaments, act as "tracks" along which transport takes place. Motor proteins, such as kinesin and dynein, transport cargo in anterograde (towards the synaptic terminal) and retrograde (towards the cell body) directions, respectively (O'Malley 2010).

These motor proteins are powered by ATP hydrolysis to generate a "walking" motion along the tracks. It is shown that kinesin and dynein are interdependent (Martin, Iyadurai et al. 1999) and may both be present on a single mitochondria (Pilling, Horiuchi et al. 2006)They are connected by adaptor complexes such as those of Miro (Fransson, Ruusala et al. 2006) and Milton (Glater, Megeath et al. 2006; Misko, Jiang et al. 2010) for the transport of mitochondria. While studies investigating the control and regulation of movement direction and speed of vesicle and mitochondria transport have begun, much remains unknown in the study of axonal transport and movement.

1.4.1 Axonal transport defects in PD

There have been many signs of disruption to axonal transport in major neurodegenerative diseases. Overexpression of α-synuclein has led to axonal transport defects (Saha, Hill et al. 2004). Pink1 and Parkin mutations have been shown to disrupt mitochondrial transport within axons (Wang, Winter et al. 2011). MPP+ has led to transport disruptions of mitochondria in giant squid axons (Morfini, Pigino et al. 2007). 6-OHDA treatment has led to destabilization of microtubules in cell-free assays (Davison, Legault et al. 1986). In PC12 cells, MPP+ has been shown to disrupt stability of microtubules, which subsequently led to the disruption of mitochondria movement (Cartelli, Ronchi et al. 2010). However, in murine mesencephalic models, mitochondrial disruption due to MPP+ occurs prior to loss of microtubule tracks. Therefore, it is still controversial which aspect of the axonal process is disturbed first (Kim-Han, Antenor-Dorsey et al. 2011). Other PD models, such as rotenone, have also shown disruptions to mitochondrial transport (Choi, Palmiter et al. 2011). Many additional questions regarding axonal transport dysfunction remain unanswered. For example, is there a dysfunction in the motor proteins which decreases their movement

efficiency? Could there be a deficiency in binding between motor proteins and their cargo or perhaps motor proteins and the tracks? Could there be an energy deficiency which precludes the function of motor proteins? A disruption to any aspect of the axonal transport machinery could lead to the activation of a program for axonal degeneration (Burke and O'Malley 2012).

1.5 Mitochondrial dysfunction in PD

Mitochondria are dynamic organelles that perform important functions such as producing energy in the form of ATP, acting buffers for regulating intracellular calcium ions, and regulating apoptosis through release of cytochrome c in response to stressors. Transport of mitochondria throughout a neuron, and its extensions such as axons and dendrites, is critical for supporting and maintaining the function of those particular compartments. The length of the axon places a heavy energy demand on the cell. Many processes within the axon rely on the energy provided by mitochondria, such as movement of the motor proteins, maintaining microtubule tracks, attachment and loading of vesicles. Disruption of mitochondria movement or limiting the distribution of mitochondria to places of high energy demand (such as at the axonal terminal) may compromise meeting the high energy requirement. Maintenance of the health of the mitochondrial network is complex and tightly regulated by fusion and fission processes to share healthy mtDNA or to sequester and break off damaged compartments within the mitochondria (Youle and van der Bliek 2012). Parkinsonism toxins have been linked to mitochondrial dysfunction since the discovery of the effects of MPP+ on complex I activity (Cleeter, Cooper et al. 1992). Other parkinsonism drugs, such as rotenone also inhibit complex I activity (Betarbet, Sherer et al. 2000). Though MPP+ induces acute parkinsonism which is different from progressive PD, post mortem studies of idiopathic PD patients have shown reduced complex I activity in the SNpc (Schapira, Cooper et al. 1990).

Interestingly, other cells, such as platelets derived from PD, patients have also shown reduced complex I activity, which may suggest a systemic defect (Haas, Nasirian et al. 1995). Damage to complex I may then contribute to disruption of ATP production and increase the formation of ROS that will lead to mtDNA damage and higher levels of oxidative stress.

1.5.1 Mitophagy

Mitochondria removal is an important process for regulating the health of the mitochondria network within a cell. The oxidative phosphorylation process within mitochondria presents a source of ROS, such as hydrogen peroxide and super-oxides, which may cause oxidative damage to lipids, DNA, proteins and other mitochondria. Damaged mitochondria may also release their inner stores of calcium ions and cytochrome c, which will lead to axonal degeneration and cell death. Therefore, it is important for normal mitochondria to be separated from the damaged mitochondria so that the health of the network is not affected and also for the damaged organelles to be sequestered and removed quickly. While several pathways exist for mitochondrial control to recycle misfolded proteins, the process for removing entire mitochondria is a selective form of autophagy (a catabolic process to degrade intracellular components) known as mitophagy. While there are three main types of autophagy: micro-, macro-, and chaperone-mediated autophagy (Mizushima and Komatsu 2011), the focus will be on the process of macroautophagy, which will remove an entire mitochondrion.

A simplified description of autophagy is as follows. First, an autophagophore will form and eventually engulf a damaged mitochondrion to form what is known as an autophagosome, which can be identified by markers such as LC3 I and II. Second, this autophagosome will be transported towards a lysosome, enriched in the cell body rather than in the axons). Finally, the autophagosome

will fuse with the lysosome to form an autolysosome, and the contents of the autophagosome will be enzymatically degraded (Tanida 2011). While autophagy is an ongoing process occurring all the time within a cell, over- or under-activation or disruption to any portion of the autophagic process could contribute significantly to the neurodegenerative disease process (Wong and Cuervo 2010). It is thought that recessive forms of PD, such as Pink (Dagda, Cherra et al. 2009)1 and Parkin (Narendra, Tanaka et al. 2008), may lead to a disrupted mitophagy process and lead to accumulation of damaged mitochondria. 6-OHDA treated animals and *in vitro* models have shown upregulation of autophagy and increased cell deaths but autophagy inhibition via 3MA (Li, Wang et al. 2011) or a constitutively active form of Akt that is part of the PI3 kinase/Akt/mTOR pathway lead to the rescue of neuronal death (Cheng, Kim et al. 2011).

1.6 Different mechanisms between axonal degeneration and apoptosis

Despite knowing the role that axonal injury plays in degenerative diseases, treatments to halt the progress of axonal die back have proven elusive (Raff, Whitmore et al. 2002). The primary reason is that degeneration of cell bodies and neurites occur via independent processes; protection of one does not guarantee protection of the other. For example, caspase 3 is not activated during axonal degeneration, but is activated during programmed cell death (Finn, Weil et al. 2000). Compared to the wealth of information available on programmed cell death or apoptosis, players involved in axonal degenerative pathways are only beginning to emerge (Osterloh, Yang et al. 2012).

A significant amount of data concerning the distinctiveness of the axons from the cell bodies comes from studies done on Wld(S) or Wallerian degeneration slow mutation (Lunn, Perry et al.

1989). This spontaneous mutation has shown to confer protection to axons and significantly delay the process of Wallerian degeneration due to various types of physical and biochemical injuries. However, this protection does not extend to the cell bodies as Wld(S) was able to confer protection against MPP+ induced axonal degeneration but did not protect the cell bodies (Hasbani and O'Malley 2006; Antenor-Dorsey and O'Malley 2012). With 6-OHDA, Wld(S) protected against anterograde models of degeneration, but did not protect against retrograde degeneration (Cheng and Burke 2010). Wld(S) has also shown protection against axotomy and microtubule destabilization via vincristine (Wang, Wu et al. 2001) in peripheral neurons (Coleman 2005). In addition to Wld(S), knockout of JNK2 and 3 have also conferred protection against 6-OHDA-induced degeneration of midbrain cell bodies but did not rescue the axons (Ries, Silva et al. 2008). Growth factor signaling led to the degeneration of neurites but left cell bodies intact (Campenot 1982; Mijatovic, Piltonen et al. 2011). The players involved the pathways underlying axonal degeneration are only beginning to be uncovered. But the lack of tools to easily and effectively study axonal processes has hampered the progress of such research.

1.7 Tools for studying Axons

The study of axonal processes, such as development, path finding and growth in the peripheral nervous system (PNS) in neurons, such as superior cervical ganglia or dorsal root ganglia, was facilitated by the use of explant cultures. Cells within the explants were able to easily survive and extend their axons. It is possible to cut and remove the cell bodies after the axons have extended to the desired length in order to have a pure axonal culture (Araki, Sasaki et al. 2004). However, the fragility of CNS neurons precluded successful explants from being established using CNS tissue. The development of the three compartmented Campenot chamber in 1977 provided

the ability to spatially and chemically isolate axons from the cell bodies led to the discovery of growth factors (such as nerve growth factor) that impacted neurite growth (Campenot 1977). Since then, various modifications or simplifications to both the Campenot chamber's design and also the microgrooves along which neurites could travel have been developed to facilitate a variety of different assays (Ivins, Bui et al. 1998).

The key to the usability of Campenot and explants in axonal experiment has been an understanding of how to elicit neurite outgrowth through the use of growth factors and culture conditions (Campenot 1987). Using single or combinations of growth factors, such as NGF or GDNF, PNS neurons show robust neurite outgrowth in *in vitro* models. However, promoting neurite outgrowth from CNS neurons remains a challenge as the axon growth and guidance pathways are less well studied compared to PNS neurons. Conditions for culturing CNS neurons must also be modified because these cells are much more sensitive and more difficult to culture than PNS neurons

1.7.1 Soft Lithography

Advances in microfabrication techniques have driven tremendous growth in the MEMS industry (Bryzek, Peterson et al. 1994). Techniques such as conventional lithographic techniques such as photolithography offered unparalleled methods in creating nano and microsized structures. In photolithography, structures are created by pouring a photoresist over a substrate (typically a silicon wafer), placing a photomask above it and then passing radiation through the mask. The areas of the photoresist exposed to the radiation would then be rendered hard and insoluble; the unexposed photoresist can then be washed away from the wafer (Rai-Choudhury 1997). However, despite the attractive feature of being able to create micron sized features, the choice of materials

and expensive costs (e.g. maintenance of clean rooms and long process times) (Geppert 1996) have limited the application of photolithography in areas of biology and medical sciences.

It was not until the development of soft lithography that the ability to rapidly and cheaply create small structures in biologically compatible materials was finally within grasp. (Zhao, Xia et al. 1997; Xia and Whitesides 1998). Soft lithography is a set of non-photolithographic techniques used to generate submicron structures. An elastomeric stamp with a pattern or structures upon its surface is used to create microstructures ranging from 30 nm to 100 μm in a process known as replica molding (Xia, Kim et al. 1996). For biological applications, polydimethylsiloxane (PDMS) is the most widely used material for generating the patterns or relief. Other materials include polyurethane and polyimides. PDMS is a liquid at room temperature but can easily be converted into a solid via a crosslinker. Typically the liquid PDMS is poured onto a patterned master, a silicon wafer with patterned photoresists created using standard photolithographic techniques, and then heated to generate a solid via a hydrosilyation reaction between the vinyl (SiCH=CH2) and hydrosilane (SiH) group (Clarson and Semlyen 1993). The elastomer makes conformal contact with surfaces of large areas and can be easily released from the master upon curing. This functionality allows for rapid prototyping and fast iterations of multiple designs. The surface structure of PDMS is quite stable and does not adhere irreversibly to many surfaces (Xia and Whitesides 1998). However, it is worth noting that the crosslinking reaction is not always complete and may require longer time, increased crosslinker to base polymer ratio, or higher temperature and pressure (such as those found in an autoclave) to drive the reaction to completion. Otherwise, oligomers would diffuse out of the bulk product and may adversely affect biological assays (Berthier, Young et al. 2012). As a material for biological applications, PDMS has other attractive features such as being optically transparent down to 300 nm, which supports use of traditional Brightfield, fluorescent and confocal microscopy. PDMS is durable and gas permeant to CO_2 and O_2, which renders it favorable

for cellular applications (Xia and Whitesides 1998). These properties make PDMS an excellent candidate for the design of and rapid prototyping of microfluidic devices.

1.7.2 Microfluidic Devices for the Study of Neurons

With the development of soft lithographic techniques by the Whiteside group at Harvard, many groups were quick to exploit the flexibility and capacity of techniques, such as replica molding and microcontact printing to design microfluidic compartments and cellular assays (Whitesides, Ostuni et al. 2001). The ability to manipulate the extracellular environment with such ease led to the development of many innovative "lab on a chip" devices that could generate gradients to study stem cell differentiation or trap and sort single cells to study cell motility or the effects of shear forces (Qin, Xia et al. 2010). These microdevices could manipulate small biomolecules, such as proteins, DNA, and RNA (Beaudet and Belmont 2008) or facilitate the study of entire organisms, such as C. elegans (Ben-Yakar, Chronis et al. 2009; Chung, Crane et al. 2009; Shi, Wen et al. 2010). One of the first microfluidic devices geared towards the study of central nervous system axons in isolation of the cell body and dendrites was first developed by the Jeon lab (Taylor, Rhee et al. 2003). This design and other similarly inspired microfluidic devices have enabled the isolation of hippocampal and cortical neurons thus overcoming the limitation of Campenot and explants for the study of CNS axons. With the microfluidic model system, Jeon was able to perform experiments on only the axons and also acquire axonal material for assays, such as the western blot or RNA extraction (Taylor, Blurton-Jones et al. 2005). However, neurons from the mesencephalic midbrain could not be cultured successfully within the Jeon microdevices (Kim-Han, Antenor-Dorsey et al. 2011). Very few neurons survived the loading process and of those that did survive, few were close to the microchannels and could extend neurites (Kim-Han, Antenor-Dorsey et al. 2011). This result

suggests that the particular design of the Jeon microfluidic device is not compatible with all neuron type of the central nervous system.

1.8 Concluding Remarks

The development of compartmented chambers that could support the growth and isolation CNS axons would greatly facilitate the study of disease causing processes. Tools, such as the Campenot chamber and explants, are limited to the study of peripheral systems. The development of soft lithographic microfluidic devices enabled the study of CNS neurons and their axonal processes. However, early device designs from the Jeon group did not allow for the study of all CNS neuronal populations, in particular DA neurons of the nigrostriatal pathway. The loss of these neurons led to the onset of motor symptoms in PD patients and understanding the degenerative process for these cells may help to better design therapies that could halt the cell death and disease progression. Therefore, the first part of this dissertation focused on the design of a microfluidic device that gave researchers the ability to study intracellular processes of midbrain DA neurons.

Since axonal degeneration and disruptions to axonal transport, are key parts of neurodegenerative diseases, the microfluidic device designed in the first part of the dissertation was used to study transport processes within dopaminergic axons and how these processes are affected when the cells are treated with a toxin, 6-OHDA that is commonly used to model PD. By studying axonal degenerative events and the order in which they occur, a clearer understanding of axonal degeneration could be obtained.

Overall, this work seeks to design a tool that would enable better study of degenerative processes within the CNS and then demonstrate the tools' application towards the investigation of a major neurodegenerative disease.

Chapter 2

Designing a microfluidic device for isolating single dopaminergic neurons

2.1 Abstract

Much experimental evidence has pointed to the importance of mitochondria transport defects in the onset of major neurodegenerative diseases, such as Parkinson's disease. Imaging of mitochondria transport along single axons is notoriously difficult with traditional dissociated culture systems, and the fragility of the midbrain dopaminergic neurons precludes their survival in microfluidic devices with an enclosed architecture. Using soft lithography, a microfluidic device was created from PDMS for the purpose of studying the transport of mitochondria along single dopaminergic axons. The device, comprised of two large chambers connected by a parallel array of microchannels, achieves separation of axons from the soma and allows tracking of mitochondria movement along oriented axons. Dopaminergic neurons from midbrain cultures were successfully cultured in the chambers and extended their axons into the microchannels. Axonal mitochondria within the microchannels were labeled by transduction with a DsRed2 lentiviral vector or with a mitochondria specific dye, Mitotracker Deep Red, and were visually tracked with conventional confocal microscopy. The methodology described here will allow study and additional understanding of the role that mitochondrial transport defects play in major neurodegenerative diseases.

Contents of this chapter were published in J Neurosci Methods 2012 June: 209(1): 35-9 and reprinted with permission of the publisher

2.2 Introduction

Parkinson's disease (PD) is the second most common neurodegenerative disorder, affecting more than 20 million people worldwide (Mayeux 2003). The major clinical symptoms of this disorder arise from the loss of dopaminergic (DA) neurons. It has been suggested that the onset of motor symptoms is due to the loss of the axonal projections to the striatum (60-70%) compared to the loss of DA cell bodies (~30%) (Cheng, Ulane et al. 2010). Support for this notion comes from recent studies showing that genes whose mutations are responsible for familial forms of PD, such as *Parkin* and *Pink1,* encode for proteins that regulate mitochondrial trafficking and impairment (Yu, Sun et al. 2011). Moreover, the PD-mimetic, 1-methyl-4-phenylpyridinium (MPP+) (Blum, Torch et al. 2001), rapidly leads to abnormal trafficking of DA axonal mitochondria and loss of mitochondrial function (Kim-Han, Antenor-Dorsey et al. 2011). However, the latter studies are currently hampered by the lack of a simple, standardized device to rapidly separate axons from cell bodies.

To study axonal transport, investigators have used versions of compartmented Campenot chambers (Campenot 1977; Ivins, Bui et al. 1998) to isolate axons from the cell body. These devices seal a piece of Teflon to a petri dish using silicone grease, and the Teflon acts as a divider to create two or more compartments; three compartments in the original Campenot and two compartments in Ivin's modified Campenot (Ivins, Bui et al. 1998). Previously, we have used Ivin's modified compartment chamber, which consists of a semicircular Teflon piece walled off at one end by a glass cover slip supported by a layer of collagen/Matrigel and sealed to a Petri dish using silicone vacuum grease (Kim-Han, Antenor-Dorsey et al. 2011; Iglesias-Gonzalez, Sanchez-Iglesias et al. 2012). Neurons were seeded on one side of the glass cover slip and extend axons through the collagen to the axonal side of the chamber (Kim-Han, Antenor-Dorsey et al. 2011). Although effective at isolating the axons from the neurons, one downside of this design and the original Campenot

chamber is that the isolated axons are randomly oriented, making it difficult to distinguish between anterograde and retrograde transport.

A major advance in axon trafficking came from microfluidic devices designed by the Jeon lab that are fabricated using soft lithographic techniques. These devices orient the axons by forcing them to grow through a parallel array of microchannels that connect somal and axonal compartments (Taylor, Rhee et al. 2006). Previous reports showed that dorsal root ganglion (Kim, Karthikeyan et al. 2009) and hippocampal neurons (Taylor, Blurton-Jones et al. 2005) can be successfully cultured in these devices. However, we have found that they are not suitable for culturing midbrain DA cultures, as the majority of DA neurons do not survive within the enclosed somal compartment, and those that remain fail to extend axons into the axonal compartment (Kim-Han, Antenor-Dorsey et al. 2011).

To overcome the limitations of previous compartmented devices and create a culture platform for investigating the role of mitochondrial transport in axonal degeneration during PD, we designed a microdevice with a large "open" compartment versus the enclosed compartments devised by Jeon lab. This "open" chamber is directly adjacent to an array of parallel microchannels that will allow us to 1) culture midbrain DA neurons 2) isolate DA axons 3) orient the axons to allow determination of retrograde and anterograde directions and 4) visualize these axons by live cell imaging so that we can record the movement of axonal mitochondria over time. One advantage of miniaturization is that we can place two devices on a single 35mm petri dish, allowing us to run more than one condition (e.g. control vs. experimental) simultaneously. Using these devices and green fluorescent protein expressing DA neurons from a line of transgenic mice (DA/GFP) (Kim-Han, Antenor-Dorsey et al. 2011), we can study the effects that PD-mimetic drugs such as MPP^+ have on mitochondrial transport and other transport processes.

2.3 Materials and Methods

2.3.1 Microdevice Designs

A summary of the process for creating a microdevice is depicted in Fig. 2.1. First a CAD file of the design for the microdevice was dawn using AutoCAD (Autodesk, CA) and used to generate high-resolution transparency masks (CAD/Art Services, OR). The microchannels and relevant surface markers were drawn in separate layers from the main compartments and its markers so that a mask was generated for each (i.e. one for the microchannels and the other for the compartments). For features below 10 μm, a glass-chrome mask (Infinite Graphics Inc, MN) was needed.

A two-step photolithographic process was then used to produce the master wafer. To prepare the surface for either 10 or 5 μm microchannels, a clean silicon 15 cm wafer (Silicon Inc, ID) was briefly washed in hydrofluoric acid, then distilled water, and then dried using nitrogen to render the surface hydrophobic. The wafer was then placed on a spin coater and SU8-2 (Microchem, MA) was poured onto the surface so that 95% of the wafer was covered. The spin coater settings to generate the microchannels are as described in Table 2.1.

	Acceleration	**Spin speed**	**Duration (s)**
Step 1	100 rpm/s	500 rpm	5
Step 2	300 rpm/s	1000 rpm	30
step 3	300 rpm/s	0 rpm	2

Table 2.1 Spin cycle settings to generate 5 μm tall microchannels using SU8 2

The wafer was then "soft" baked at 65ºC for 1 minute and then baked 95ºC for another minute. Then the wafer was placed onto the mask aligner with the microchannel pattern and exposed to UV for 8 seconds. After exposure, the wafer was baked again at 65 and 95ºC for 1 minute each. The

wafer was then placed into a container filled with SU 8 developer (Microchem) and gently swirled for 12 minutes to remove excess SU-8 2. The wafer was hard baked at 195ºC for 12 minutes to remove cracks and imperfections.

The second step was to generate the main compartments. The procedure is similar as to what was previously described for making the microchannels. The differences are that SU 8 2050 (Microchem) was used as the photoresist. The protocol for the main compartment spin cycle is shown in Table 2.2.

	Acceleration	**Spin speed**	**Duration (s)**
Step 1	100 rpm/s	500 rpm	5
Step 2	300 rpm/s	1500 rpm	30
step 3	300 rpm/s	0 rpm	2

Table 2.2 Spin cycle settings for 100 μm tall main compartments using SU8 2050

The soft bake after spin coating was 65 and 95ºC at 5 and 12 minutes, respectively. The UV exposure time was increased to 20 seconds. After exposure, the wafer was baked at 65 and 95ºC for 5 and 8 minutes, respectively and then developed using SU 8 developer for 12 minutes. As in the microchannel step, the wafer was hard baked at 195ºC for 12 minutes.

After the wafer has been constructed, the master underwent a silanization process by placing a small drop of trichloromethylsilane (TCMS) (Sigma-Aldrich, MO) on a 35 mm dish lid next to the wafer in a desiccator. The TCMS was vaporized and deposited onto the wafer so that the PDMS did not stick to and destroy the wafer. After silanization, the wafer was ready for use.

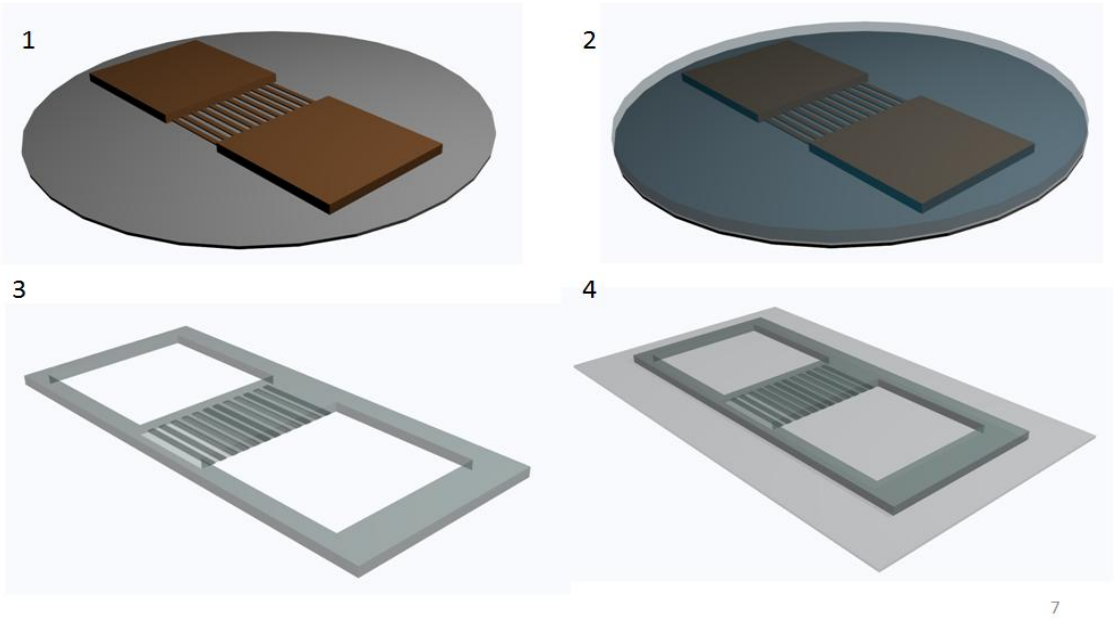

Figure 2.1 Outline of Replica Molding Process. 1) A master wafer with negative photoresist is created using standard photolithographic techniques. 2) An elastomer is poured over the master. 3) After the elastomer crosslinks, the microdevice is cut out. 4) The microdevice is bonded to a glass cover slip for cell culture

2.3.2 Replica Molding

PDMS in the form of Sylgard 184 (Dow Corning, USA) was mixed vigorously for 10 minutes at a ratio of 10:1 (base : curing agent) to ensure a homogenous mixture, and poured over the wafer. Then, the mixture was placed into a vacuum desiccator and the gas was evacuated in order to remove air bubbles trapped during mixing. The chamber was evacuated periodically to speed up the bubble removal process. Afterwards, the PDMS was baked overnight at 60ºC to solidify the PDMS piece. Higher temperatures at shorter time periods were ruled out to avoid warping the polystyrene dish containing the wafer. After the PDMS had been solidified via

crosslinking, it was cut out of the dish and then autoclaved at 125ºC for 25 minutes. Microdevices treated through the autoclave process showed fewer instances of unpolymerized PDMS oligomers diffusing in the culture medium and healthier cells (Berthier, Young et al. 2012).

To create the main compartments, a 6 mm diameter Visipunch (Huot Instruments, USA) was used. One side of the Visipunch was flattened against a table top to create a linear edge, punching out an opening that would expose as many microchannels as possible. A punch farther away from the opening of the microchannels would create an overhanging space that resists fluid flow and cell deposition, unnecessarily limiting the number of cells that could be placed next to the microchannels and the number of neurites able to extend into these microchannels.

The base for the cut out PDMS microdevice was a 35mm dish with a 23mm diameter hole cut out from the bottom. A thin (0.09-0.12mm) glass cover slip (Carolina Biological, NC) was attached to the bottom of the cut out dish. This set up renders the device amenable to use on an inverted confocal microscope. After the microdevice was cut out and the compartments were punched, the devices were cleaned thoroughly using scotch tape and a compressed air blower to remove dust and debris. Reproducible and successful bonding (fewer leaks between compartments) required dry and clean surfaces. The microdevice was irreversibly bonded to the glass coverslip dish via air plasma treatment (Harrick Plasma, USA) for two minutes at a high setting. Having an irreversible seal improved fidelity of the bond and decreased the "leaks" that may occur between compartments when feeding or plating due to accidental bumping of the microdevices. The finished microdevices were then coated with poly-D-lysine (PDL) (Sigma-Aldrich, MO) at 0.2 mg/mL overnight and sterilized via UV treatment for 30 minutes in a standard flow hood. After 24 hours, the microdevices were washed three times with sterile distilled water and left overnight within the incubator. Two hours prior to cell plating, the microdevices were filled with DMEM+ plating

media, which was comprised of DMEM/F-12 (Sigma-Aldrich), B-27 (1:50 dilution) (Invitrogen), penicillin and streptomycin (Invitrogen) and 5% fetal bovine serum (FBS, Sigma-Aldrich).

2.3.3 Midbrain Cell Culture:

DA/GFP cultures were harvested from Tg(TH-EGFP) DJ76GSAT transgenic mice (Jackson Laboratories, ME). These mice were created by mating a DA/GFP male with a wild type female. The midbrain was isolated from pup embryos on embryonic day 14 (E14) and then screened for GFP fluorescence prior to dissection. All GFP positive tissues were pooled.

Isolated neuronal culture were then plated within the somal compartment at 60,000 cells per well. For plating, the cells were also concentrated by spinning in a centrifuge so that the final loading volume per well was 5 μL. The smaller loading volume increased the likelihood that most of the cells were loaded closer to the microchannels and not distributed throughout the compartment. On DIV 5, the media was supplemented with AraC (Sigma-Aldrich, final concentration: 5- 10 μM) to limit the proliferation of glial cells. On DIV 2, the cells were transitioned to feeding with fresh neural basal media (neural basal supplemented with glutamine (Sigma-Aldrich) and B-27) every two or three days to ensure that fluid levels within the microdevices were maintained. The microdevices, prone to evaporation, were checked for fluid levels every other day. When feeding, additional media (15-20 μL more) was added to replace what was lost due to evaporation. The thickness of each microdevice ranged from 0.7 to 1.5 cm and each compartment was filled with approximately 100-120 μL of media. To induce axonal extensions, Netrin I (300 ng/mL, R&D Systems, MN) was added as a supplement to the axonal compartment starting on DIV 5 with every feed.

2.3.4 Mitochondrial Labeling

Lentiviral labeling

A mitochondrially-targeted DsRed2 was generated by inserting a mitochondrial targeting sequence from complex IV of the mitochondrial electron transport in front of the DsRed2 (Clontech) (Araki, Sasaki et al. 2004). The mitoDsRed2 was then subcloned into a FUGW lentiviral expression vector provided by Dr. Jeffrey Milbrandt (Washington University in St. Louis). The lentivirus was generated in HEK293T cells and collected using an Optima LE-80K Ultracentrifuge (Beckman-Coulter, USA). Viral concentration was titrated so that approximately 70-80% of cells expressed mitoDsRed2. The lentivirus was added to the midbrain cultures in the microdevice on DIV2 for 5-6 hours.

Mitochondrial Dye Labeling.

Mitochondria were also labeled with Mitotracker Red and Deep Red (Invitrogen) at recommended concentrations of (25 nM and 50 nM respectively) either 30 minutes prior to imaging or 24 hours prior to imaging on DIV 13 or 14. With 24 hours of labeling, a higher concentration of dye was used (~100 nM for only 15 minutes), and then the cells were washed and left to incubate over night.

2.3.5 Confocal Imaging.

Time lapse images of mitochondrial movement were taken using a Zeiss LSM510 Meta NLO Multiphoton System (Carl Zeiss) on Axiovert 200M inverted microscope with a 40x water objective [C-Apochromat 40x/1.2W Corr.1.2 numerical aperture, collar correction (0.14-0.18)]. The

microscope contains a heated stage which includes a Pecon CTI-Controller 3700 for regulating 5% CO_2 (Zeiss, USA) and a Pecon TempControl 37-2 digital (Zeiss) for heating the stage to 37ºC for the duration of the image recordings. A total of sixty images of mitochondrial movement at 5 s intervals were recorded and then used to generate kymographs for measurement of transport.

Filters used for visualizing the fluorescent markers included a 488 nm argon laser and 505 longpass emission filter (GFP), 543 HeNe laser and 560 long pass emission filter (MitoDsRed2 and Mitotracker Red) and a 633 nm HeNe laser and 650-710 bandpass emissions filter (MitoTracker Deep Red FM).

2.3.6 Immunocytochemistry

Primary midbrain cultures were plated within the microdevices and then fixed on DIV12-13. Cells were washed twice with PBS, fixed with 4% paraformaldehyde for 20-25 minutes, and then washed three times with PBS for 15 minutes per wash. To visualize dendrites and axons, cultures were stained with mouse β-tub-III IgG2a (Millipore, MA) and mouse MAP2 IgG1(Millipore) primary antibodies (1:2000 and 1:1000 dilutions respectively). Secondary antibodies used were goat anti-mouse IgG2a Alexa488 (Invitrogen) and donkey anti-mouse IgG1 Alexa647 (Invitrogen) at 1:500 dilutions. Blocking was done using Roth blocking buffer (1% bovine serum albumin, 0.2% milk, 0.3% Triton X100). To allow for sufficient penetration of antibodies into the microchannels, all blocking and antibody incubations were done overnight. Typical antibody incubation times (e.g. 2 hours with secondary antibodies and 1 hour of blocking) produced inconsistent antibody staining within the microchannels and only the cells and axons within the larger compartments showed consistent staining.

2.3.7 Kymograph Analysis of Moving Particles

Kymographs generated using ImageJ (NIH, Bethesda, MD) were analyzed as described previously. Time lapse images were imported into ImageJ and then the image was split into individual channels. A threshold image of the mitochondrial channel was used for analysis. A segmented line was then used to select the region of interest. An add-on to ImageJ called Multiple Kymographs was then used to generate each kymograph derived from the region of interest. Each diagonal line upon a kymograph represented a moving particle while the straight lines represented nonmoving particles. The angle and length of each line was then used to calculate the direction and speed of the moving mitochondria. To convert between the pixels and lengths/times, the following equations were used:

$$\text{Distance } (\mu m) = (112.5 * (\text{Length} * \text{COS}[\text{RADIANS}(\text{Angle})]))/ 512 \quad (2.1)$$

$$\text{Time } (s) = 5 * (-\text{Length} * \text{SIN}[\text{RADIANS}(\text{Angle})]) \quad (2.2)$$

The following parameters were used: 112.5 was the frame length, 512 was the pixel size of the image, and 5 was the interval between images. Only particles that moved more than 5 μm in length for at least 15 seconds were counted as motile.

2.3.8 Modeling toxin diffusion:

Transport of MPP^+ into the somal compartment of a Jeon microfluidic device (approximated by a rectangular block that is 7 mm in length, 1.5 mm in width, and 100 μm in height) was modeled as a convection-diffusion problem using COMSOL multiphysics software version 4.0a (COMSOL Inc, Burlington MA). The concentration of MPP^+ within the compartment was initially

set to zero and the concentration of the MPP^+ at the entrance of the compartment was set to 2 μM. The model assumed diffusion through water at 37°C and a diffusion coefficient of 1 μm/ms.

2.3.9 Statistical Analysis:

One way ANOVA and unpaired two-tailed Student's t-tests were used for statistical analysis (Statistica). P value below 0.05 was considered as statistically significant.

2.4 Results

2.4.1 "Open compartment" microdevice shows improved viability and axon growth for midbrain DA/GFP neurons.

Trying to culture midbrain DA neurons within the Jeon microfluidic device proved unsuccessful. The somal compartment of the Jeon device is enclosed within the PDMS and plating/feeding the cells within the compartment is done through two large wells connecting directly to the somal compartment. But after repeated attempts, it was found that very few of the midbrain cells remained within the somal compartment of the Jeon device (Fig 2.2A), and most of the cells were found within the larger loading wells away from the microchannels. The cells that remained within the somal compartment did not survive. It is possible that even with careful technique and extended plating time, shear forces that occur during loading may damage the fragile midbrain cultures and may remove them from the somal compartment. Additionally, the somal compartment of the Jeon device holds only a very small volume of culture media; hence it may take a long time for nutrients to diffuse from the media compartment to the cell compartment and for waste to diffuse out. Also, dead cells are trapped within the cell compartments and cannot be removed after plating without risking further shear damage to the surviving cells. Finally, the enclosed nature of the device makes toxin treatment of DA axons or cell bodies difficult as excessive force may dislodge the cells. Because some PD toxins oxidize within a few minutes, rapid, homogeneous delivery of toxin is critical for consistent results. Modeling diffusion of 2 μM MPP^+ through an enclosed somal compartment show that uneven distribution of the toxin at 1 hour (Fig. 2.2B).

A

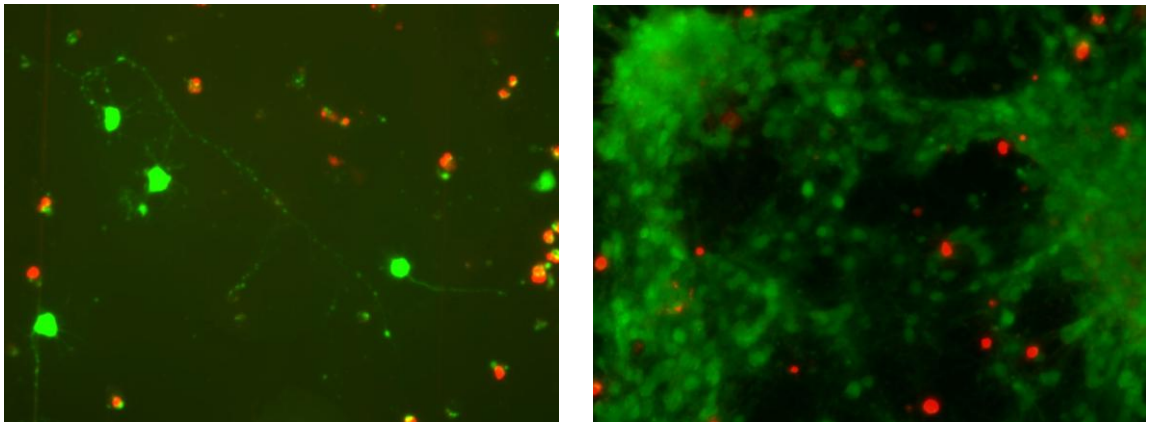

B

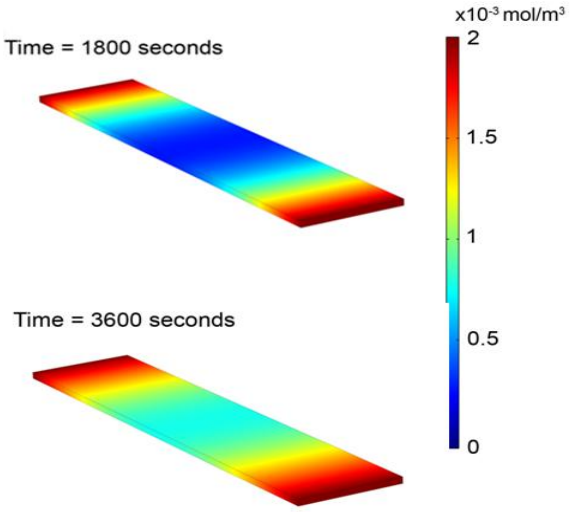

Figure 2.2 Midbrain cultures survive within open compartmented microdevice A) Representative images of live dead assay performed on midbrain neuronal cultures plated within Jeon microdevice (left) and open compartmented device (right)Very few healthy cells remained within the Jeon microdevice on DIV 5 while cultures survival very well within open compartmented microdevices. B) COMSOL simulation of diffusion of 2 μM MPP+ into cellular compartment of Jeon microdevice showed that even after 1 hour of diffusion, concentration has not equilibrated.

An "open" compartmented microfluidic device was designed for the culture and isolation of midbrain axons (Fig 2.3A). The decision behind the design was to mimic the "openness" of the compartmented chamber described by Ivins (Ivins, Bui et al. 1998) while combining the array of parallel microchannels for aligning and orienting axons. This open design enabled direct access to and loading of the cells right next to the microchannels for convenient cell seeding, media sampling, cell/axon labeling and more efficient waste/nutrient exchange. The new design also reduced

exposure of the cells to shear forces during plating and feeding, and ensures that the cells have sufficient access to a large volume of media through the entire culture period.

A

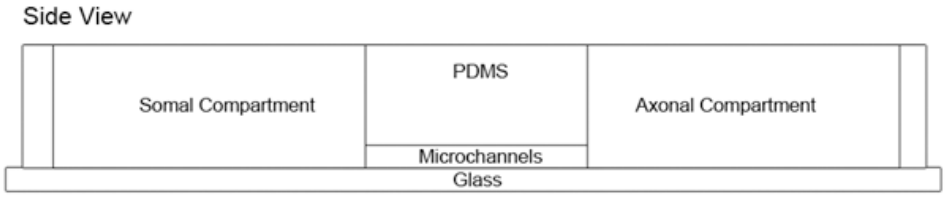

B

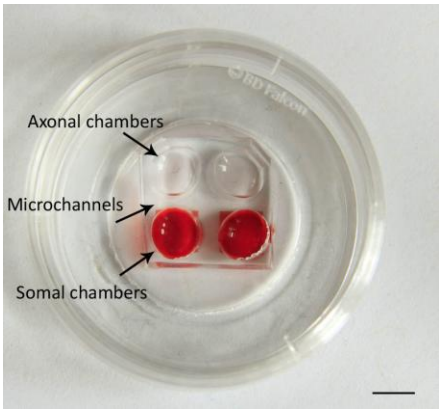

Figure 2.3 Schematic of Microdevice. A) Each microdevice is composed of two open compartment connected by an array of 237 microchannels. The dimension of the microchannel in the final microdevice design is 500 x 5 x 5μm (l: w: h) B) Two microdevices can fit onto a single 3 5mm dish. A 23 mm (diameter) hole was cut and Corning glass cover slip (0.09-0.12 mm thickness) was adhered to the bottom of the dish using PDMS. Fluidic isolation was maintained using a 30 μL volume difference between the axonal and somal chambers. Scale bar indicates 5 mm.

60,000 cells per well were chosen as the final loading density for each compartmented chamber. Higher cell densities (100,000 per well) exacerbated the problem of axonal bundling and made obtaining single axons difficult. Lower densities (40,000 cells per well) limited the number of axons that could extend into the microchannels. Two different microchannel widths (10 and 5 μm) were tested to try to obtain the maximal number of singly aligned isolated axons. Axonal bundling in microdevices with 10 μm was significant and very few (2-5) of the microchannels had single axons per device. Use of devices with 5 μm microchannels and adjusting the amount of virus used to

transduce 70-80% of cells significantly improved the probability of obtaining single labeled axons in each microchannel.

Axons begin extending into the microchannels by DIV 6 and on DIV 10-12 would completely cross the microchannels into the axonal compartment. The microchannels between the somal and axonal compartments provided both a means for orienting axons as they extend and for providing fluidic isolation between the compartments so that drugs can be applied separately to either the axons or cell bodies. This isolation is maintained by a hydrostatic pressure difference created by a volume difference (~30 μL) between the compartments. A large proportion (~30%) of microchannels contained DA/GFP axons so that imaging of mitochondria from many different neurons is possible. Based on morphological assessments, there was no evidence of dendrite infiltration in the micro-channels, nor did neurites in the axonal chamber stain for the dendritic marker MAP2 (Fig. 2.4A). Using the open chamber microdevice, DA/GFP cultures were successfully plated and maintained for up to 4 weeks (Figure 2.4B). Over time (>DIV14), axons continued to fasciculate such that establishing directionality and uniqueness became problematic. Thus measurements of mitochondrial movement were performed on either V13 or 14.

A

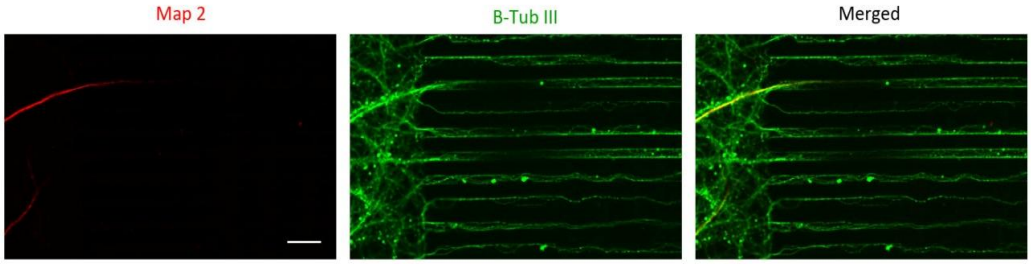

B

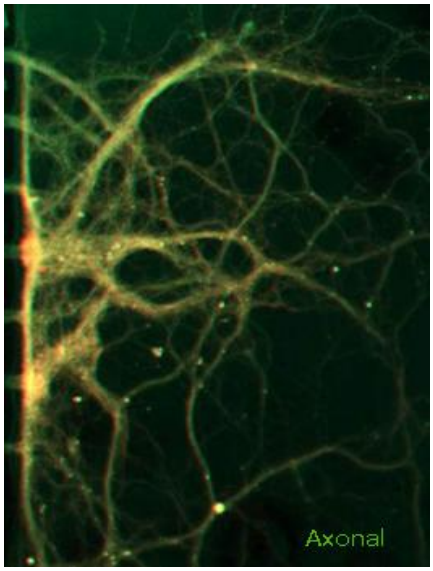

Figure 2.4 Isolation of axons within axonal compartment A) Dendrites (labeled with MAP2 antibodies) do not extend significantly into the microchannels by DIV 14 so that the population of neurites (β-tubulin-III staining) extending into the axonal compartment is purely axons. B) Midbrain cultures can be maintained within the microdevice for long term studies. Depicted in B are axons with mitochondria labeled with by DsRed2 and stained with β-tub III at DIV 27.

A major advantage of the open chamber system is that the microchannels "straightened" the axons making distinguishing between anterograde and retrograde movement very simple. No axon was observed to reverse directions within the micro-channels to grow toward the somal compartment. The alignment provided by the microchannels is a significant improvement compared to the random growth of the axons in the Campenot compartments. In the Campenot, the axons are often likely to cross other axons and change direction (i.e. growing back towards the somal

compartment), making it difficult to identify the transport direction even when using landmarks, such as the growth cone. Establishing polarity is important for understanding the disruption of axonal transport processes, as anterograde and retrograde transport are mediated by different proteins and may be targeted in different ways during degeneration. Previously, we found a difference between anterograde and retrograde transport of mitochondria after exposure to MPP^+. Specifically, there is a decrease in anterograde transport speed and an increase in retrograde transport speed. These data are consistent with a model in which impaired mitochondria stop traveling towards the growth cone and instead return to the cell body for repair. A culture platform that allows for the isolation of aligned axons and visualization of interior transport processes can aid the process of addressing the mechanisms underlying these events.

2.4.2 Mitochondria of oriented DA/GFP axons can be tracked and measured within microchannels.

Using an optically transparent and biologically compatible elastomer, PDMS, it is possible to visualize and track the movement of mitochondria in live cells by either transducing the cells with the mitochondrial-targeted DsRed2 lentiviral vector (Fig. 2.5)

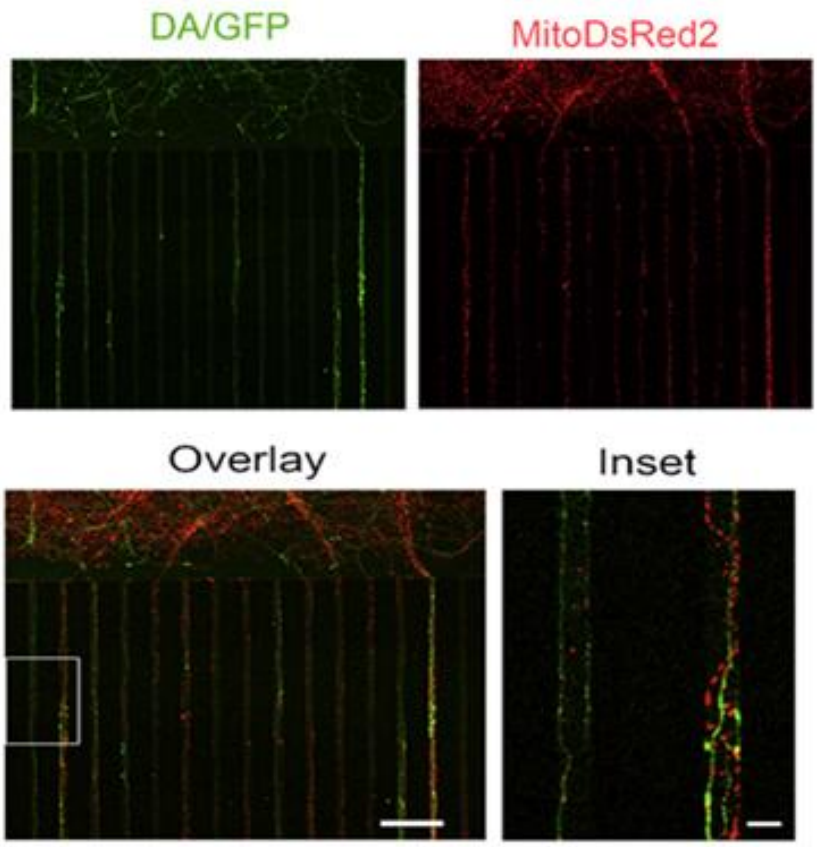

Figure 2.5 Axonal mitochondria can be clearly tracked within microchannels. GFP expressed under a tyrosine hydroxylase promoter identifies and shows the extensions of DA axons into the microchannels. Mitochondria labeling that do not co-localize with GFP staining show the bundling of many axons within the 10 μm microchannels.

In the case of MitoDsRed2, the level of transduction can be manipulated by using varying amounts of virus so that not all of the axons within a microchannel are labeled We did not observe toxicity with either the viral or dye method of labeling, and there were no changes to the mitochondria morphology or transport speed (not shown). MitoDsRed2-labeled mitochondria were observed and tracked visually by DIV 5 in the microchannels. Alternatively, MitoTracker Deep Red labeled organelles in both somal and axonal compartments within 15 minutes. However, mitochondria labeling inside of the microchannels was not immediately apparent. The latter required incubating the cells with the dye for 20 minutes, washing out the excess dye and then letting the cells

incubate overnight in order to label the mitochondria within the microchannels. In addition, MitoTracker Deep Red tended to adhere to PDMS, and rendering it fluorescent (Fig. 2.6).

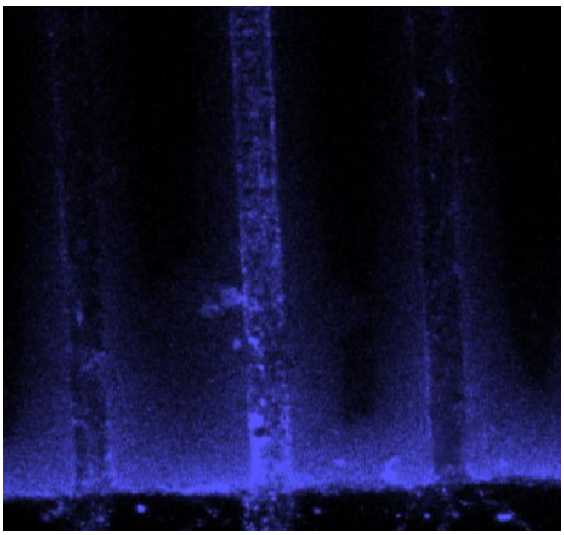

Figure 2.6 Disadvantage of using fluorescent dye for labeling mitochondria in microdevice. Mitotracker Deep Red was absorbed into the bulk material of PDMS and generated significant noise when visualizing and making quantitative measurements of mitochondria movement.

This leads to background noise in the channels, which can make distinguishing individual mitochondria difficult. Reducing dye concentrations did not overcome the problem but instead led to inconsistent labeling. In contrast, MitoDsRed2 had no "noise" problems and once labeled, the mitochondria could be clearly tracked within the microchannels using a confocal microscope. Time lapse images of mitochondria movement along DA axons were then used to generate kymographs (Fig. 2.7A). These kymographs were used to calculate the proportion of moving mitochondria (Fig 2.7B.) and the speed of mitochondria moving in either the anterograde or retrograde direction (Fig. 2.7C). Measurements of these key DA mitochondria parameters, such as motility, were essentially the same between the Campenot chamber (Kim-Han, Antenor-Dorsey et al. 2011) and the microdevice (21±2.3%). Mitochondria speeds between the two devices were also comparable to what was previous reported: anterograde speeds in the microdevice was 0.39±0.03 μm/s while the retrograde speed was 0.34±0.03 μm/s.

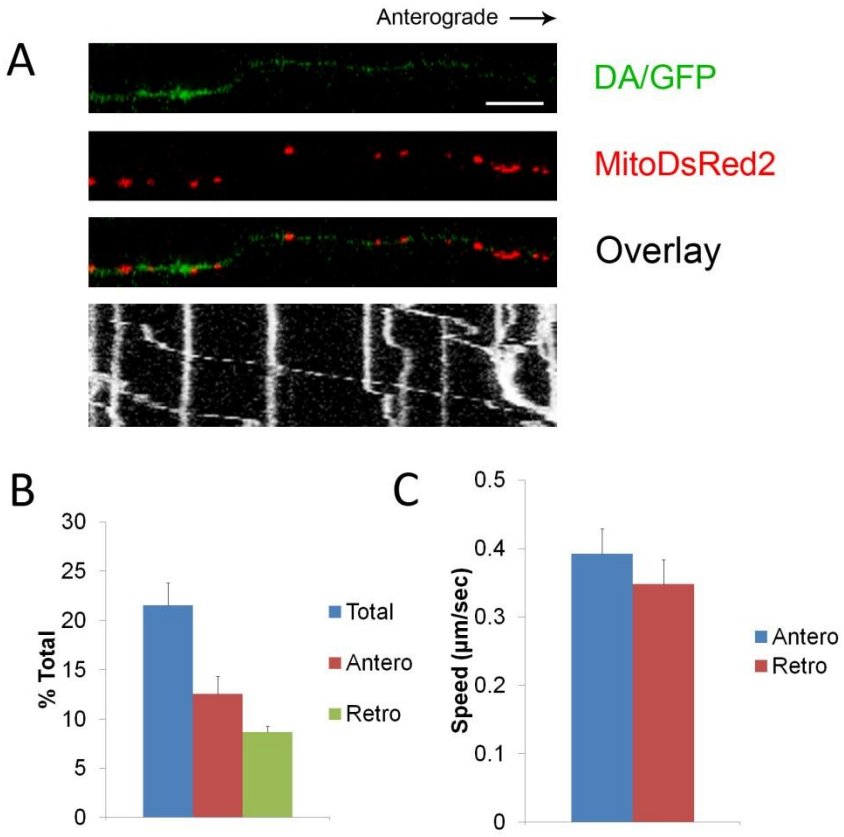

Figure 2.7 Properties of mitochondrial transport can be measured within microchannels. (A) Kymograph of mitoDsRed2 labeled DA mitochondria movement within the microchannels under normal culturing conditions. Scale bar indicates 10 µm. (B) The kymographs were then used to calculate the proportion of moving mitochondria from 12 axons over 3 independent experiments as well as the (C) mitochondrial movement speed in both anterograde and retrograde directions (over 60 mitochondria were examined). Error bars indicate standard error of mean (SEM) for B and C.

2.5 Discussion

Since the development of soft lithographic microfluidic devices for culturing CNS neurons by the Jeon group (Taylor, Rhee et al. 2003), many publications have explored the application of this and other compartmented microfluidic device configurations in areas of neuroscience and neuroengineering. Electrophysiological recordings of axons using patch clamp and microfluidic

devices were possible using a modular design consisting detachable and re-sealable PDMS layers (Jokinen, Sakha et al. 2013). The key aspects of modular design include being able to use upright microscopes with microdevices and enabling access of patch clamp electrode to the cells. The thick PDMS piece often precludes focusing of the lens upon the cells and requires the use of an inverted microscope. Typically, microfabricated devices aimed at performing electrophysiology require the use of a microelectrode array (MEA) below the PDMS piece in order to perform electrophysiological recordings in slice cultures (Berdichevsky, Sabolek et al. 2009) or dissociated sympathetic neurons (Takeuchi, Nakafutami et al. 2011).

To study the responses of neuronal culture to diffusible molecules derived from glial cells, a co-culture platform was developed in which a pressure valve was used to allow or block fluid exchange between different types of cells (Majumdar, Gao et al. 2011). Modifications of this pressure valve design to additional or vertically aligned chambers allowed for the study of glial influences on neuronal synaptic formation (Shi, Majumdar et al. 2013). In addition to these co-culture devices, synaptic function could be studied in the Jeon microdevice, which has been modified with the addition of a perfusion channel that intersects with the microchannels (Taylor, Dieterich et al. 2010).

Isolation of axons within individual compartments also allowed for the study of axonal properties such as myelination (Park, Koito et al. 2009). Using a diffusible gradient generator, the Folch group has studied the response of axon guidance and turning in response to diffusible factors (Bhattacharjee, Li et al. 2010). Femtolasers and patterned surface proteins have also been used in conjunction with microfluidic neuronal devices study axonal pathfinding and axonal regeneration (Kim, Karthikeyan et al. 2009; Shi, Nedelec et al. 2010; Hur, Yang et al. 2011).

Microfluidic devices have also been used as model systems for neurology to investigate studying Alzheimer's disease (Kunze, Meissner et al. 2011; Kim, Park et al. 2012), spread of exogenous alpha-synuclein fibrils for PD (Volpicelli-Daley, Luk et al. 2011), as well as the spread and transport of herpes simplex and rabies virus in neurons (Liu, Goodhouse et al. 2008). Despite the potential that soft lithography and microfluidic devices hold to investigate many important questions in biology or medical sciences, widespread use of microfluidic devices in biological research has not yet occurred. In the history of cell culture, the application of microfluidics to areas of biology remains within its nascent stages. Many technical challenges such as material selection and device geometry need to be addressed to ensure a standardized, easy to use and consistently performing product that the engineers can then pass onto biologists. The challenges and difficulties associated with each biological problem are unique and modifications to a microfluidic device design may be necessary. For example, as was presented in this research, an enclosed compartment design for a microfluidic culturing platform does not support the growth of DA neurons and therefore cannot be used for the study of axonal processes.

The methods provided by the results of this research provide a convenient and easy technique for real time tracking and measurements of axonal transport processes within DA axons. In summary, the methods presented by this research provide a technique for real time tracking and measurement of the movement of labeled mitochondria in oriented DA axons. This technique could be extended to the study of other processes, such as vesicular transport and microtubule fragmentation, which may also participate in the onset of axonal degeneration. The microdevice platform shown here displays improved culture conditions for sensitive neurons, such as those from the midbrain and promotes oriented axon growth into a separate axonal compartment for analysis. Using this culture system, it is possible to obtain a better understanding the mechanisms of axonal

degeneration that may underlie the pathophysiology of major neurodegenerative diseases, such as Parkinson's disease.

Acknowledgements

The authors would like to thank Steve Harmon for his help in the cell harvest and Dennis Oakley for technical assistance during imaging. This work was funded by NIH grants R21 NS067561(SSE) and NS39084 (KOM).

The authors declares no conflict of interest

Chapter 3

The Effects of 6-OHDA on Axonal Transport

3.1 Abstract

6-hydroxydopamine (6-OHDA) is one of the most commonly used toxins for modeling axonal injury and understanding degeneration of dopaminergic (DA) neurons in Parkinson's disease. But how 6-OHDA causes axonal degeneration and affects intra-cellular processes, such as axonal transport, is still unknown. To investigate the response of axons to 6-OHDA, a microfluidic device designed to isolate axonal processes was used to separate DA axons labeled with green fluorescent protein (GFP) from their cell bodies. The axons were treated with 6-OHDA and transport processes were then examined. 6-OHDA quickly induced mitochondrial transport dysfunction in both GFP and non-GFP labeled axons. We also observed disruption in transport of synaptophysin-tagged vesicles. These toxin effects on mitochondrial transport were blocked by the addition of SOD1-mimetic, Mn(III)tetrakis(4-benzoic acid)porphyrin chloride (MnTBAP), as well as the anti-oxidant N-acetyl-cysteine (NAC). However, addition of calcium ion chelator, ethylene glycol tetraacetic acid (EGTA), did not restore mitochondrial transport. The results from the study suggest that transport dysfunction occur early and may play a significant role in inducing axonal degeneration in response to 6-OHDA treatment.

3.2 Introduction

Axonal degeneration plays a critical role in the development of major neurodegenerative diseases, such as Parkinson's disease (PD) (Coleman 2005). The cardinal motor symptoms of PD, bradykinesia, resting tremors, postural instability, and limb rigidity are associated with the loss of dopaminergic (DA) neurons that are part of the nigrostriatal pathway. The cell bodies of these neurons reside within the substantia nigra, and they innervate areas of striatum, such as caudate and putamen where they play a role in the regulation of motor function (Dauer and Przedborski 2003). Functional imaging and patient studies have indicated a significant loss of striatal dopaminergic terminal fields prior to the loss of cell bodies (Riederer and Wuketich 1976; Lee, Samii et al. 2000). *In vivo* models with PD toxin, such as MPP+ (Fuller and Hemrick-Luecke 1985) and 6-OHDA have also been shown to induce significant axonal injury(Kirik, Georgievska et al. 2004). Autosomal dominant genetic models of Parkinson's, such as α-synuclein, have shown similar patterns of axonal pathology (Orimo, Uchihara et al. 2008).

A common feature seen in axonal degeneration is disruption of axonal transport. Mitochondrial movement was severely interrupted by the expression of mutated Pink1 and Parkin, which are responsible for two familial forms of early onset PD (Wang, Winter et al. 2011). In giant squid axons, MPP+ quickly disrupts mitochondrial transport in the anterograde direction while increasing transport in the retrograde direction (Morfini, Pigino et al. 2007). In murine dopaminergic neuron cultures, MPP+ showed similar trends of lowering overall mitochondrial motility and an increase in the speed of retrograde mitochondrial transport within 30 minutes of treatment. Mitochondria were also damaged as indicated by the loss of mitochondrial membrane potential (Kim-Han, Antenor-Dorsey et al. 2011). This effect was limited to dopaminergic neurons, as MPP+ is selectively transported via the dopamine transporter (Blum, Torch et al. 2001). Synaptic

vesicle and other particle transport was unaffected by MPP+. It is hypothesized that MPP+ induces toxicity via a thiol-redox mechanism because N-acetylcysteine, a glutathione precursor, as well as glutathione itself were able to abolish the effects of MPP+ and rescue the cell bodies and neurites. In addition, NAC has also been shown to protect against MPP+-induced decreases in mitochondrial motility. Interestingly, the use of other general antioxidants, such as SOD1 mimetic, MnTBAP, and calcium chelator, EGTA, did not rescue dopaminergic axons and neurons from the effects of MPP+ (Kim-Han, Antenor-Dorsey et al. 2011). In 6-OHDA models, NAC, catalase, super-oxide dismutase (SOD) and SOD mimetic, such as MnTBAP were observed to attenuate the degree of DA cell death (Kulich and Chu 2003; Holtz, Turetzky et al. 2006; Saito, Nishio et al. 2007; Iglesias-Gonzalez, Sanchez-Iglesias et al. 2012).

The disruption of mitochondrial transport due to MPP+ was one of the earlier events seen in mouse midbrain neurons. It wasn't until 3 hours post-treatment when a significant rise in the number of autophagosomes was observed, and it took more than 6 hours to observe a significant increase in the number of fragmented microtubules (Kim-Han, Antenor-Dorsey et al. 2011). This study and others thus suggest that mitochondrial transport and dysfunction leads to other transport defects, such as the destabilization of microtubule tracks (Kim-Han, Antenor-Dorsey et al. 2011). *In vitro*, studies of PD patients' fibroblasts (Cartelli, Goldwurm et al. 2012), differentiated PC12 cells (Cartelli, Ronchi et al. 2010), and *in vivo* murine studies (Cartelli, Casagrande et al. 2013) have indicated that MPP+ also acts as a destabilizing factor for microtubules (Cappelletti, Pedrotti et al. 2001; Cappelletti, Surrey et al. 2005) and could disrupt trafficking. In these models, the microtubules destabilized prior to loss of mitochondrial transport due to MPP+. Resolving this conflict in whether transport is disrupted before or after microtubule destabilization will be important in understanding the order of events that leads to axonal degeneration.

To study axonal degenerative processes, we previously developed a microdevice that allowed for the compartmentalization of neuronal segments so that we can isolate and orient single axons from the dendrites and cell body(Lu, Kim-Han et al. 2012). Using this device, we have studied the effects of 6-OHDA on various axonal transport processes within murine mesencephalic cultures. In addition, we have also investigated mechanisms that may underlie 6-OHDA-induced axonal degeneration.

3.3 Materials and Methods

3.3.1 Microfluidic device and cell culture

Microfluidic devices were fabricated and cell culture studies were performed as previously described in chapter 2 of this dissertation.

3.3.2 Optical Imaging

Mitochondria labeling and time-lapse images with mitoDsRed2 was performed the same as previously described in chapter 2. A lentivirus used to label synaptic vesicles was created as previously described (Araki, Sasaki et al. 2004) using a plasmid containing synaptophysin fused in frame with cerulean (provided by Dr. Rachel Wong, University of Washington Seattle). DA/GFP cultures were transduced with the virus on DIV 2 for 5 hours. Time lapse images for both vesicle and mitochondrial transport were taken as previously described in chapter 2. A 458 nm argon laser with 466-514 meta emissions filter set was used in conjunction with a 488 nm argon laser and 505 long pass emissions filter to identify vesicle transport.

3.3.3 Image analysis

Mitochondrial transport, as well as synaptic vesicle transport, was analyzed using the methods described in Chapter 2. Particle sizes used for measuring mitochondrial dimensions (mitochondria labeled with mitoDsRed2) were generated using particle analysis in ImageJ using a threshold image.

Microtubule Structure: The integrity of microtubule was determined by immunostaining with antibodies against tyrosine hydroxylase (TH) (Pel-Freeze Biological) and acetylated tubulin (AcTub; Sigma). TH positive axons with three AcTub breaks or more were considered damaged and counted as the percentage total of all TH-positive axons.

Mitochondrial membrane potential: Cells were loaded with 25 nM of Tetramethylrhodamine ethyl-ester (TMRE, Invitrogen) for 25 minutes prior to imaging. TMRE is a positively charged cell permeant dye, which can be sequestered in healthy mitochondria due to their relative negative charge. Depolarized mitochondria with less membrane potential do not sequester TMRE and leading to a decrease in the dye intensity. Changes in mitochondrial membrane potential were determined by differences in TMRE membrane potential along an axonal region of interest before and after treatment with 6-OHDA.

Autophagy: Cultures without DA/GFP labeling were taken from the same Tg(TH-EGFP) mice (Jackson Laboratories, ME) as previously described in chapter 2. These cells were taken from pup embryos (E14), which were not positive for DA/GFP. On DIV5, cells plated within microdevices were transfected with a GFP-tagged LC3 expression vector provided by Dr. Chris Weihl (Kuma, Matsui et al. 2007). 24 hours after transfection, cells were treated with 6-OHDA for the specified

time, fixed, and then immunostained with a rabbit anti-TH antibody. A Cy3-conjugated secondary antibody (Jackson ImmunoResearch) was used to visualize TH positive cells. Images were taken using the Zeiss LSM510 Meta NLO Multi-Photon System (Carl Zeiss) on Axiovert 200M inverted microscope with a 40x water objective. Cells with LC3-GFP granules were then counted and compared to the total number of LC3-GFP positive cells.

Retrograde degeneration study: On DIV13, the axonal compartment was treated with 6-OHDA and then cell death was assayed using propidium iodide labeling at 24 and 48 hours. Fluorescent and Brightfield images were taken of cell bodies within 350 μm of the microchannel opening in the somal compartment. Cell death was quantified using the fraction of propidium iodide positive cells.

3.3.4 Statistical Analysis

Statistical analysis was performed using Statistica (Statsoft). One way ANOVA and Student's t-test were used to determine statistical significance. P values below 0.05 were determined to be statistically significant.

3.4 Results

3.4.1 Mitochondrial movement decreased in DA and non-DA axons

Axonal bundling is a natural process that presents a technical challenge when imaging particle transport within a single axon. Axons from different neuronal populations extend at different rates and axons with a slower extension rate may wrap around and follow a leading axon. With microchannel width of 10 μm, we found that there was a significant amount of bundling within each microchannel and acquiring a single axon for imaging presented a logistical difficulty. Therefore we sought to limit the number of axons present within each microchannel and increase the number of microchannels available so that we will have a higher probability of finding singly labeled axons. Previously, Peyrin et al (Peyrin, Deleglise et al. 2011) had found that reducing microchannel diameters to smaller than 3 μm had an adverse impact on the health of the axons despite limiting the number of axon per channel to around 4. Therefore, we selected 5 μm as the microchannel width, reduced the separation between each microchannel to increase the the total number of microchannels available. To label mitochondria, we used a lentivirus carrying a mitochondrially targeted DsRed2 sequence. By tittering the virus used per transduction to obtain 60-70% transduction efficiency, we saw many more singly labeled axons per microchannel.

A dose response study to assess the effects of 6-OHDA indicated that within 30 minutes, lower concentrations of 6-OHDA (20 and 40 μM) did not significantly affect the transport of mitochondria in DA axons from murine mesencephalic cultures (data not shown). At 60 μM of 6-OHDA, there was a significant decrease in axonal mitochondrial motility or the percentage of mobile mitochondria in both anterograde and retrograde direction after 30 minutes of treatment 6-OHDA within the axonal compartment and thus this concentration was used for subsequent axonal

assays (Fig 3.1A,B) However, of the mitochondria that were still motile, there was no significant differences in transport speed in either direction (Fig 3.1C). Taking advantage of the fluidic isolation between the somal and axonal compartment, experiments were performed where only the somal compartment was treated with 6-OHDA to observe the effect that an anterograde model of degeneration would have on axonal mitochondrial transport. After 30 minutes, mitochondrial motility or movement speed within the microchannels showed no statistically significant change compared to the control under this condition. 6-OHDA is popular for inducing reproducible damage to dopaminergic neurons within the nigrostriatal pathway *in vivo*. However, its auto-oxidation such as p-quinones and ROS species such as hydrogen peroxide, 6-OHDA may exert its toxic effect via an extracellular mechanism without the need for uptake via the dopamine transporter (Hanrott, Gudmunsen et al. 2006) and therefore affect non-DA cells *in vitro*. Assessment of mitochondrial transport in nonGFP axons supports 6-OHDA non-specificity as there was a significant decrease in total mitochondrial motility without an effect on mitochondrial transport speeds in either direction (Fig 3.2).

A

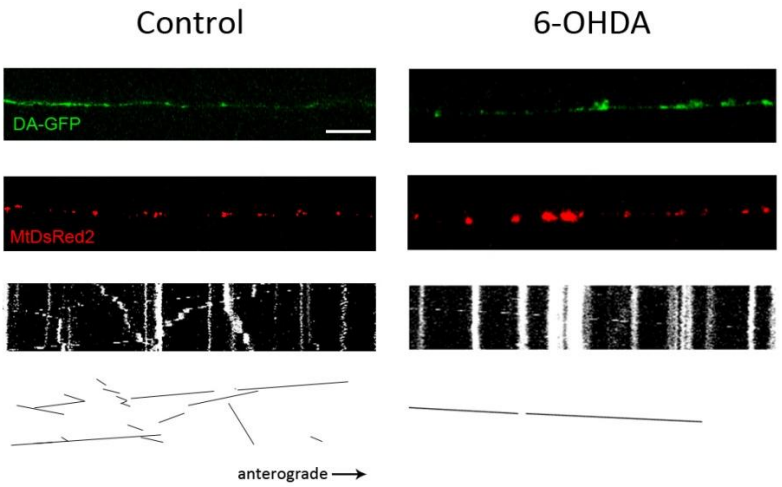
Control
6-OHDA
DA-GFP
MtDsRed2
anterograde

B

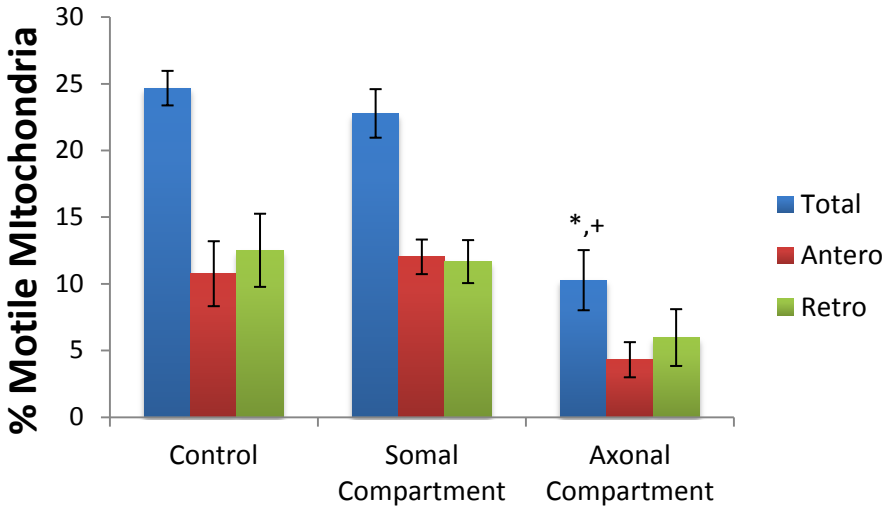
% Motile MItochondria
30
25
20
15
10
5
0
*,+
Control
Somal Compartment
Axonal Compartment
Total
Antero
Retro

C

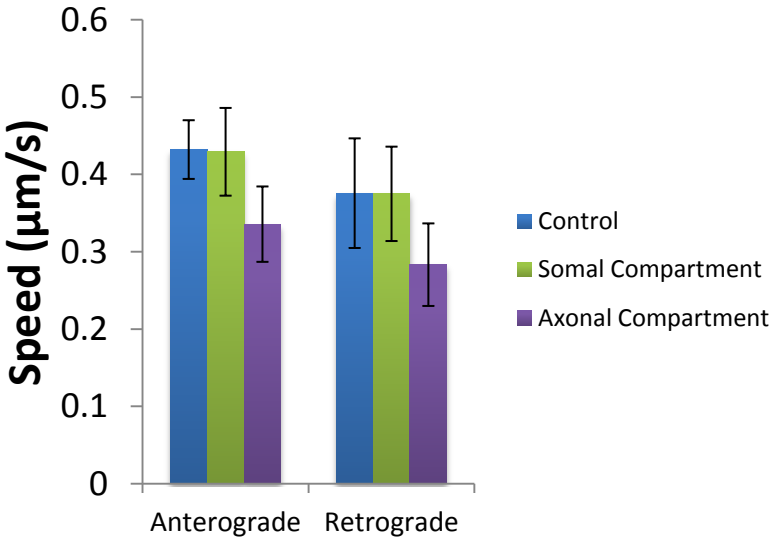
Speed (µm/s)
0.6
0.5
0.4
0.3
0.2
0.1
0
Anterograde
Retrograde
Control
Somal Compartment
Axonal Compartment

Figure 3.1 6-OHDA decreases mitochondrial movement in DA axons. A) Kymographs of axonal mitochondrial movement in control and treated axons. Mitochondria was labeled MitoDsRed2 vector and imaged 30 minutes after treatment with 6-OHDA. Quantification of B) total moving mitochondria (n = 4-5 devices per group with 4-5 axons analyzed per dish) and C) mitochondrial speeds (n = 60-80 mitochondria per group). In B and C, data is represented as Mean ± SEM, *,+ indicate $p < 0.05$ versus control and somal compartment respectively.

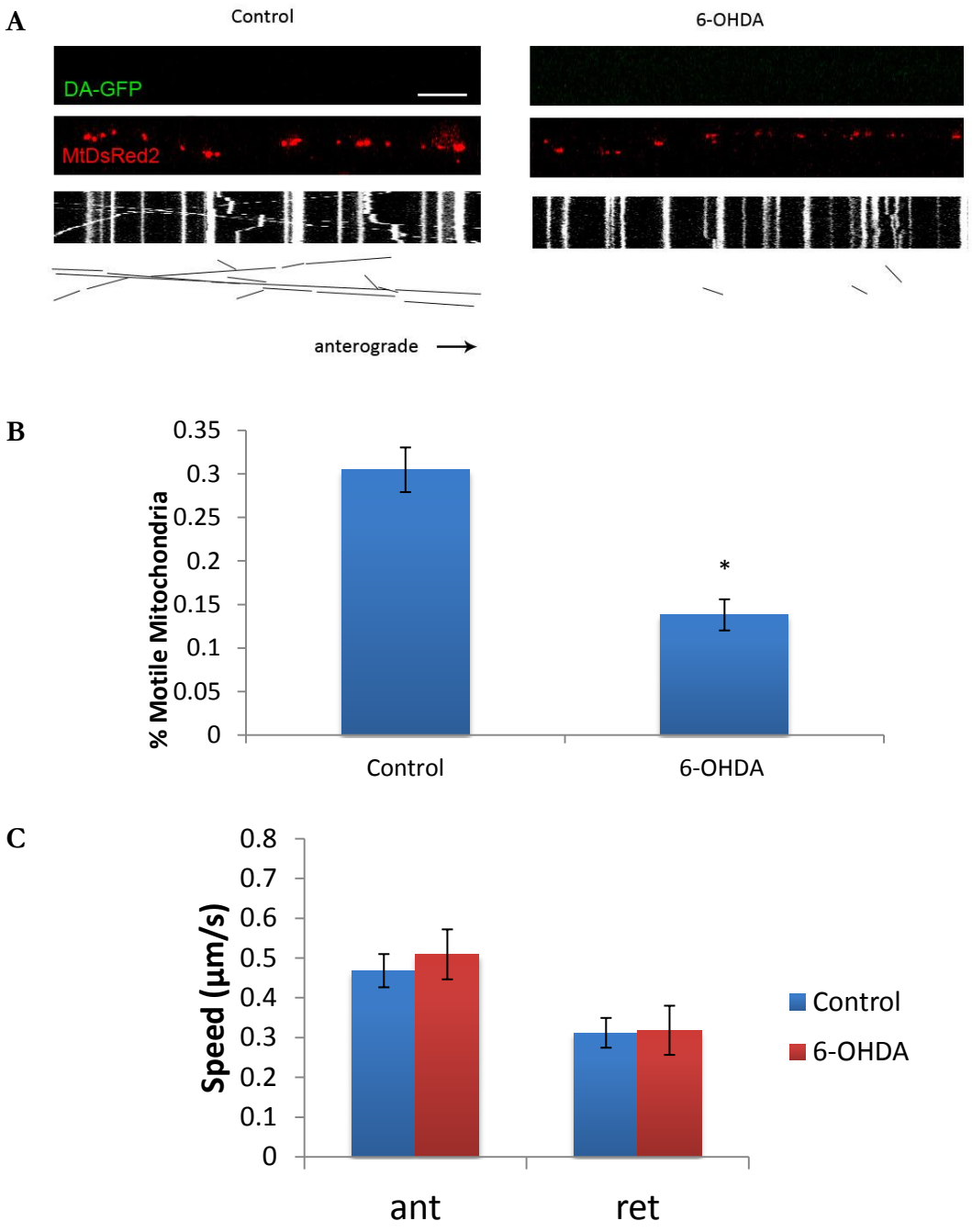

Figure 3.2 6-OHDA decreases mitochondrial movement in non-DA-GFP axons. A) Kymographs of axonal mitochondrial movement in control and treated axons. Mitochondria was labeled MitoDsRed2 vector and imaged 30 minutes after treatment with 6-OHDA in the axonal compartment. Quantification of B) total moving mitochondria (n = 20-25 axons per group) and C) mitochondrial speeds (n = 90-120 mitochondria per group). In B and C, data is represented as Mean ± SEM

3.4.2 6-ODHA damages microtubules tracks after 6 hours

Previously, it was observed *in vitro* that 6-OHDA induced a significant amount of DA cell death via apoptotic mechanisms within 24 hours. Prior to the loss of cell bodies, there was loss of DA neurites that indicates the presence of a dying back mechanism of cellular degeneration. To study the degeneration of axons at earlier time points, the structural integrity of microtubules was assessed after treatment with 6-OHDA. Cytoskeletal structures, such as neurofilaments and in particular microtubules, act as the primary tracks along which vesicles and organelle transport occur. It is conceivable that loss of these microtubule tracks would immobilize movement along axons. To determine, whether the decrease in mitochondria and synaptic vesicle movement was due to destabilization of these tracks after treatment with 6-OHDA, DA cultures were stained for acetylated tubulin, which is a marker for stabilized microtubules. No significant fragmentation in DA-GFP axons was observed until after 6 hours of treatment with 6-OHDA in the axonal compartment (Fig 3.3A). A significant amount of fragmentation in non-DA-GFP axons was also observed and followed the same time course of degeneration as observed for DA axons. By 24 hours, more than 80% of all axons assessed within the axonal compartment showed significant breaks and punctate acetylated tubulin staining (Fig 3.3B).

A

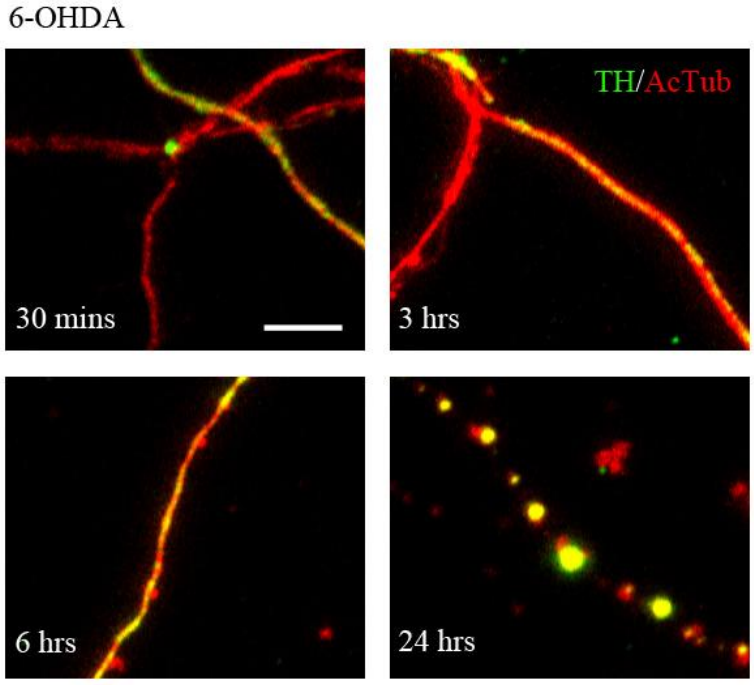

B

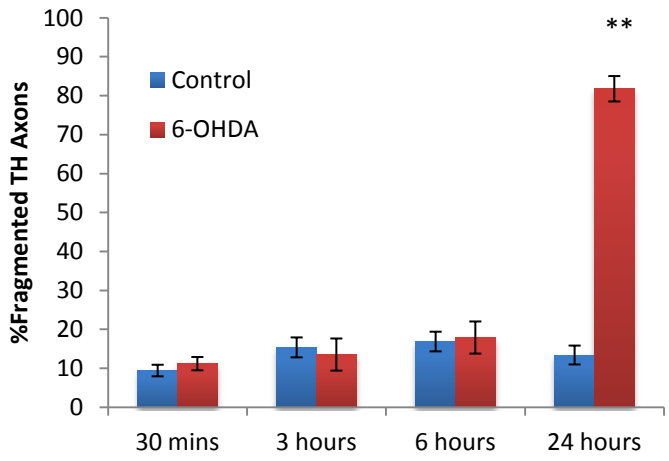

Figure 3.3 Fragmentation of microtubules after 6-OHDA treatment. A) Dissociated midbrain cultures were treated with 60 μM of 6-OHDA at the indicated times and then fixed and stained with antibodies against AcTub and TH. Significant fragmentation of AcTub is seen at 24 hours. B) TH positive axons with fragmented AcTub staining were quantified. One hundred to three hundred DA-GFP axons were counted per dish and 4-5 dishes were used per group. Scale bars indicate 10μm. Bars show Mean ± SEM. ** indicates $p < 0.001$

3.4.3 6-OHDA induces retrograde degeneration

In vivo, 6-OHDA is often used to induce retrograde axonal degeneration and commonly used as a toxin to test the efficacy of therapies for protecting DA neurons. To assess whether this form of retrograde degeneration also occurs *in vitro* and to determine when a significant degree of somal degeneration would occur, 6-OHDA was applied only to the axonal chamber and cell death was assayed with propidium iodide. No significant cell death was observed in the somal compartment until 48 hours after treatment with 6-OHDA (Fig. 3.4).

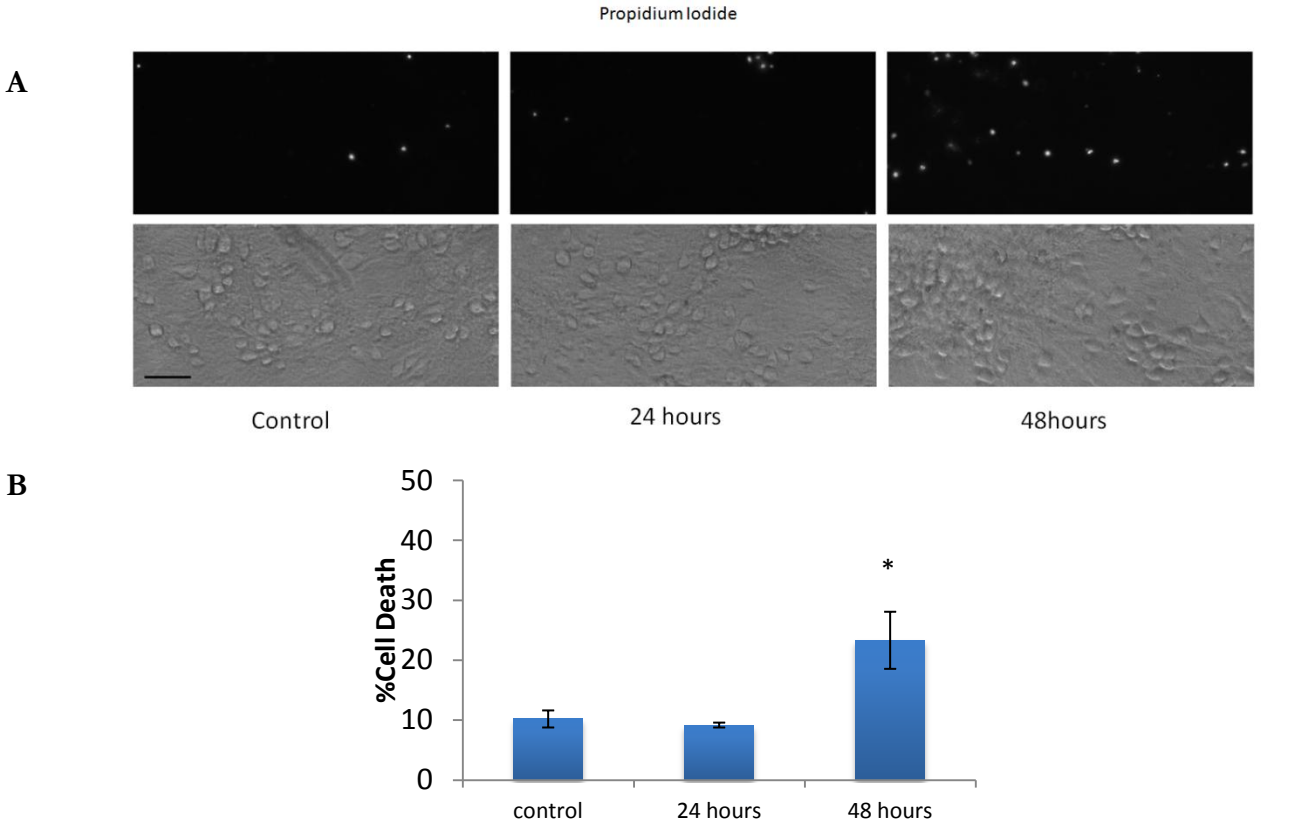

Figure 3.4 6-OHDA induced retrograde degeneration. A) dissociated midbrain cultures were treated with 6-OHDA for the indicated times and then assayed with 1 μg/ml of propidium iodide to assess cellular degeneration. B) Quantification of cell death using propidium iodide. n = 4 devices per group. Scale bar indicates 40 μm. Data is represented as Mean ± SEM, * indicates $p < 0.05$

3.4.4 6-OHDA leads to drop in mitochondrial membrane potential but does not affect mitochondrial size

Mitochondrial membrane potential is a commonly used parameter for determining mitochondrial health and may act as a signal to regulatory machinery that would lead to cessation of mitochondrial movement. Therefore to assess relative changes to mitochondrial membrane potential, we investigated the ability of mitochondria to accumulate a membrane voltage sensitive dye, TMRE and determined membrane depolarization by a decrease in TMRE fluorescent intensity. Thirty minutes after treatment with 6-OHDA, a significant decrease in TMRE fluorescence was observed in both DA-GFP axonal mitochondria and non-GFP mitochondria (Fig 3.4). To determine whether mitochondrial fragmentation plays a role in cessation of movement, mitochondrial cross-sectional area was measured using particle analysis. As TMRE fluorescence is lost upon membrane depolarization, it cannot be used to accurately measure changes to relative mitochondrial morphology. Instead, mitoDsRed2 was used to measure mitochondrial size but there was no significant difference between cross-sectional areas of the control or 6-OHDA-treated groups at 1 hour (Fig 3.6).

A

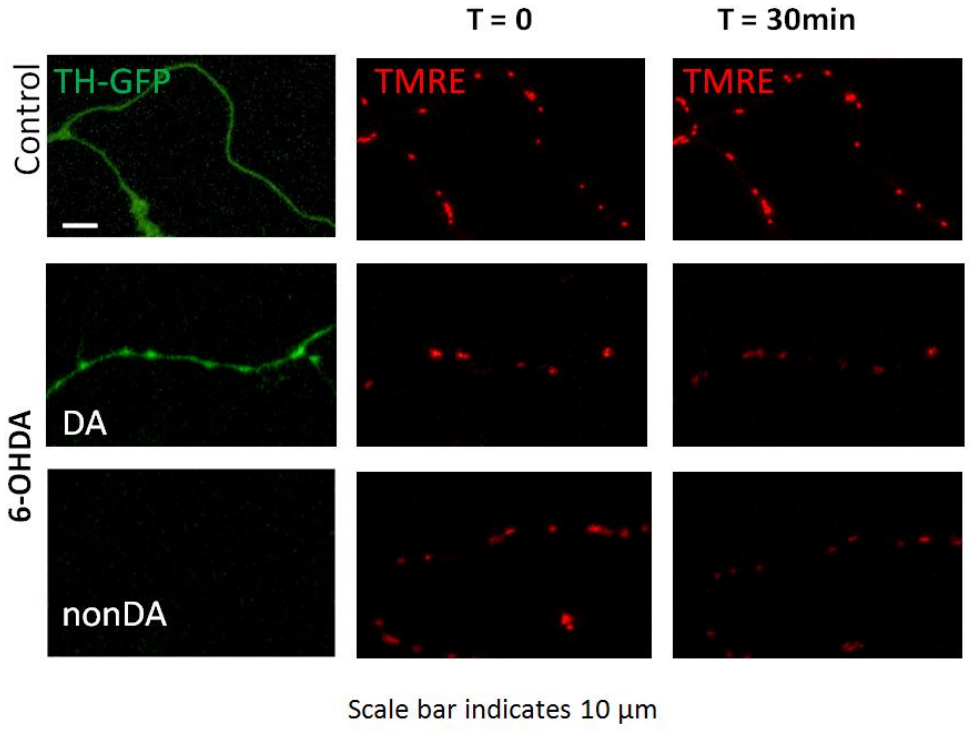

B

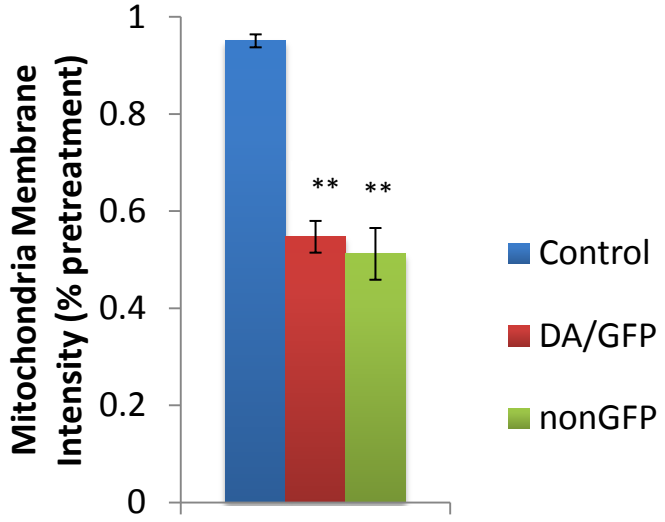

Figure 3.5 6-OHDA depolarizes mitochondria in both DA and nonDA axons. A) mitochondria labeled with 25 nM of TMRE were assessed before and after treatment. B) 6-OHDA significantly decreased mitochondrial membrane potential in axons. Data indicate Mean ± SEM from three independent experiments. ** indicate $p < 0.001$ versus control.

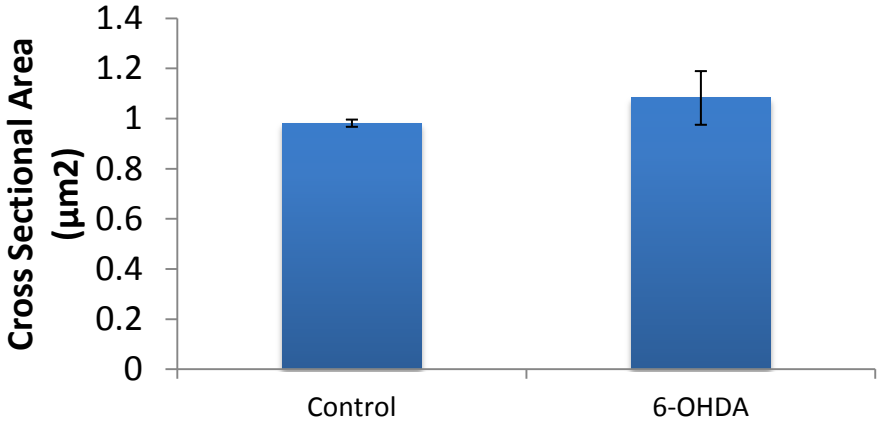

Figure 3.6 Mitochondria size unaffected during transport block. Quantification of cross-sectional area of DA mitochondria before and after treatment with 6-OHDA. Data indicate Mean ± SEM

3.4.5 6-OHDA decreases axonal transport of synaptic vesicles

To determine whether 6-OHDA specifically disrupts mitochondrial transport or whether it may affect transport of other axonal cargo, movement of synaptic vesicles was also assessed by tagging them with a synaptophysin-cerulean marker. The synaptophysin sequence had been previously shown to not co-localize with mitochondria (Kim-Han, Antenor-Dorsey et al. 2011). Similar to the decrease in mitochondrial motility, 6-OHDA significantly reduced the movement of synaptic vesicles in both the anterograde and retrograde direction after 30 minutes (Fig 3.7). Unfortunately, due to the low number of moving particles, meaningful velocity data could not be obtained from measuring the remaining motile particles. This decrease in synaptic vesicle motility show that unlike other PD-mimetic toxins such as MPP+ which specifically affects mitochondria but not other moving particles (Kim-Han, Antenor-Dorsey et al. 2011), 6-OHDA could affect additional transport machinery and decrease overall axonal transport.

A

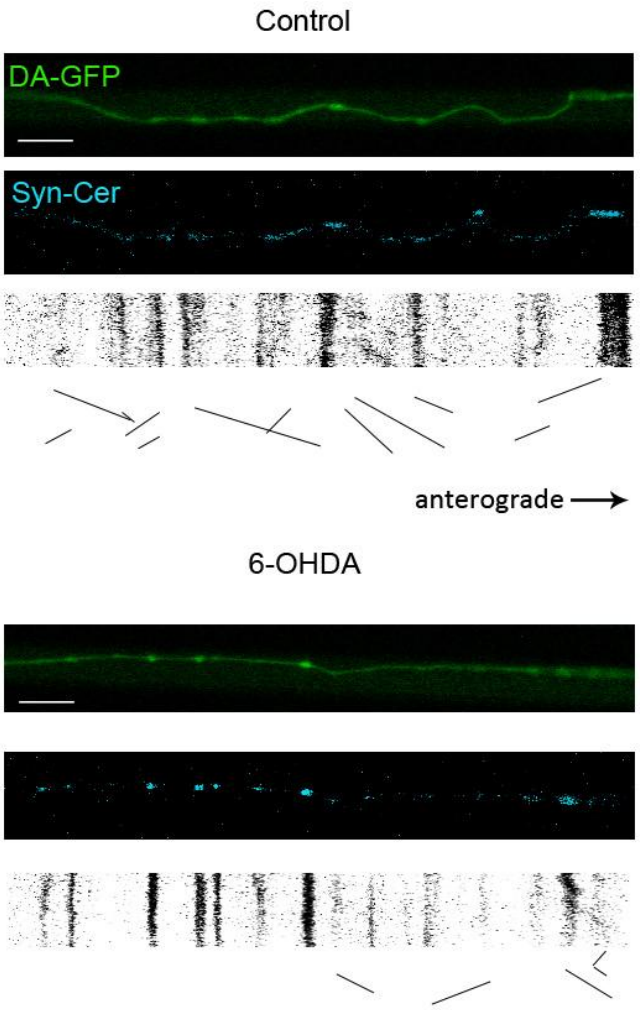
Control
DA-GFP
Syn-Cer
anterograde
6-OHDA

B

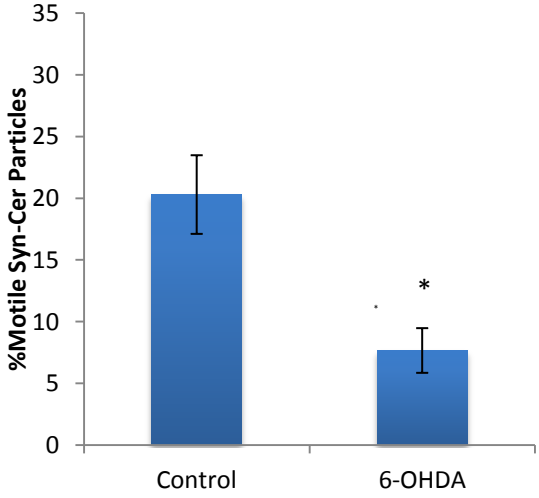
%Motile Syn-Cer Particles
35
30
25
20
15
10
5
0
*
Control
6-OHDA

Figure 3.7 6-OHDA decreases synaptic vesicle movement in DA axons. A) Kymographs of synaptic vesicle movement in control and treated axons. Quantification of B) total moving vesicles (n = 8 axons per group). Scale bar indicates 5 μm.* indicate $p < 0.05$ versus control.

3.4.6 6-OHDA induces autophagosome formation

Damaged mitochondria can release harmful levels of ROS and can be degraded by a form of autophagy known as mitophagy. Successful removal of damaged mitochondria is critical for maintaining axonal health and limiting secondary damages. Improper regulation of the mitophagy process could adversely affect neuronal health. Previously, 6-OHDA has been shown to induce autophagy in rat models (Cheng, Kim et al. 2011) and cell lines (Li, Wang et al. 2011). To determine whether 6-OHDA could also induce autophagy within murine mesencephalic neurons i*n vitro*, the appearance of an autophagy marker, LC3 or microtubule associated protein 1, light chain 3 was assessed. An LC3-clone was transfected into midbrain cultures and under control conditions, LC3-GFP take on a continuous fluorescence appearance within the cytosol. However, by 9 hours after treatment with 6-OHDA, LC3 could be seen to aggregate to the membranes of autophagosomes as suggested by the formation of LC3-GFP punctas (Fig. 3.8).

A

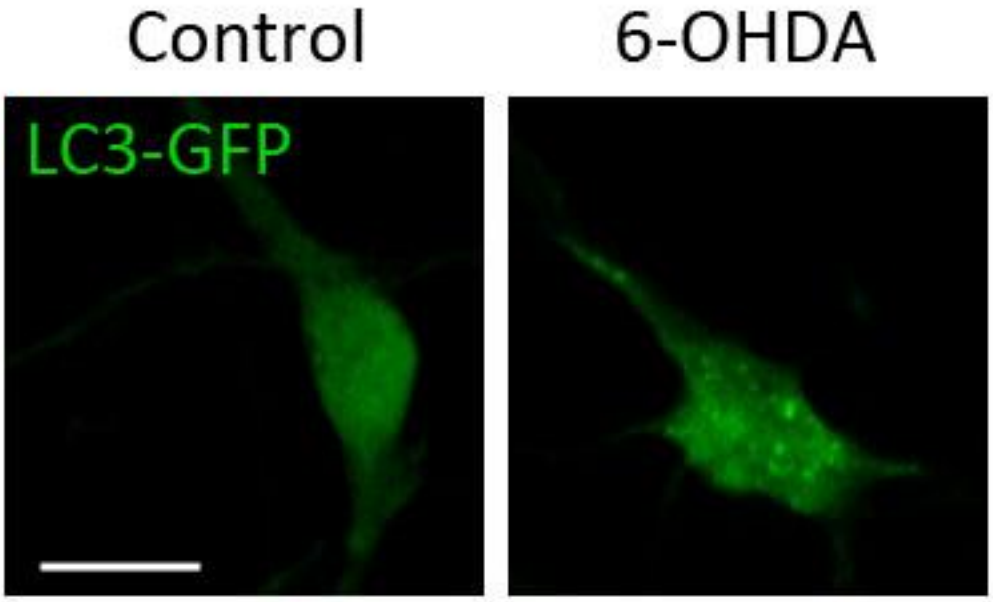

B

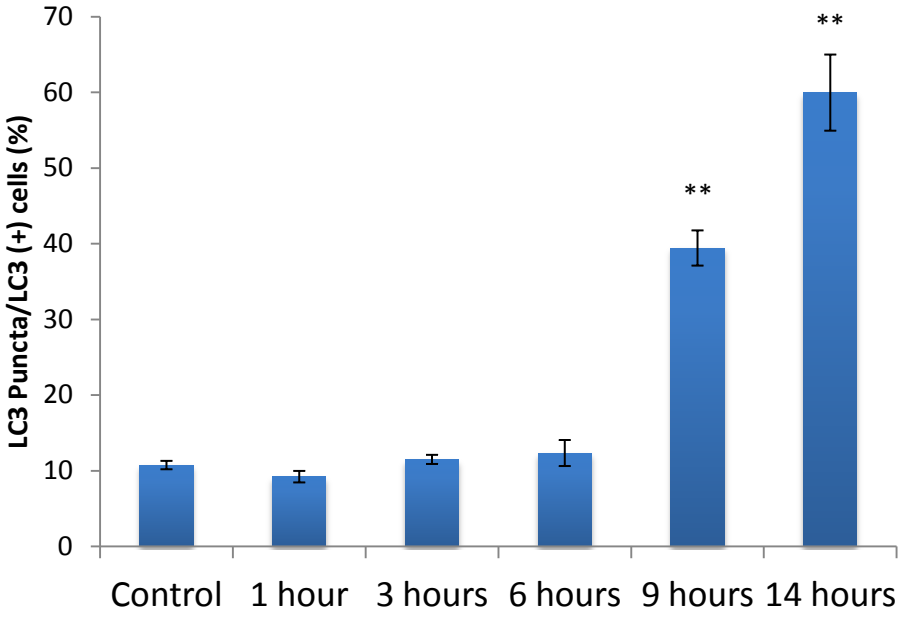

Figure 3.8 6-OHDA induces autophagy in midbrain cultures. A) Formation of autophagosomes was measured by the appearance of LC3-GFP punctas B) the number of cells with at least 3 LC3 punctas were counted and expressed as the percentage of all cells that were positive for LC3-GFP. Mean ± SEM from 4 independent experiments. ** indicates $p < 0.001$ versus control, Scale bar indicates 10 μm.

3.4.7 NAC and MnTBAP rescues mitochondrial transport

6-OHDA has been shown to inhibit mitochondrial complex I activity (Glinka and Youdim 1995) and has been suggested to induce cell death via oxidative stress primarily by increased ROS formation (Blum, Torch et al. 2001). It has also been found that ROS scavengers were potent in protecting cell bodies against the toxic oxidative byproducts of 6-OHDA (Choi, Yoon et al. 1999). To investigate whether oxidative stress induced by ROS formation also plays a role in disrupting axonal transport of mitochondria, we investigated whether anti-oxidants such as NAC and MnTBAP could rescue this early event in axonal degeneration. In addition, we also investigated whether EGTA could rescue mitochondrial transport disruption as Ca signaling plays an important role in axon degeneration (Wang, Medress et al. 2012). From table 3.1, it was found that both NAC and MnTBAP managed to protect against the transport dysfunction of mitochondrial in DA axons after treatment with 6-OHDA. However, EGTA did not protect against this loss of mitochondrial mobility.

	Motile Mitochondria
Control	24.6 ± 1.3%*
6-OHDA	10.3 ± 2.2%
NAC	25.7 ± 3.3%*
MnTBAP	28.2 ± 6.5%*
EGTA	8.34 ± 3.9%

Table 3.1 Effects of antioxidants and calcium chelator on 6-OHDA disrupted DA mitochondrial transport, data indicates mean ± SEM. * indicate $p < 0.05$ versus 6-OHDA. [NAC] = 2.5mM, [MnTBAP] = 100 μM, [EGTA] = 2.5 Mm

3.5 Discussion

From the results of the study, we conclude that unlike MPP+ which specifically affects DA neurons' axonal transport processes *in vitro*, 6-OHDA reduced mitochondrial motility in both DA and non-DA axons. Compared to other non-transport studies, a relatively high concentration of 6-OHDA was used in order to observe a difference in the motility within an hour. Lower concentrations could have been used, but it would have been logistically difficult to acquire a sufficient number of samples with longer incubation times because only one dish can be treated and imaged at a time for assessing transport. The total assessment time for each dish is about 1.5-2 hours. While 6-OHDA is known to induce apoptosis and axonal degeneration, it is not known just how it activates these pathways remain unknown. Both intracellular and extracellular mechanisms have been proposed that required or did not require the presence of DAT (Blum, Torch et al. 2000; Hanrott, Gudmunsen et al. 2006; Redman, Jefferson et al. 2006). However, for transport studies, a higher concentration is required to observe an effect therefore, it is conceivable that at the concentration used for the study, 6-OHDA acted both intracellularly after being taken up via DAT and extracellularly by oxidizing to ROS species.

Similar to MPP+, 6-OHDA induced mitochondrial depolarization and subsequent decrease in mitochondria movement is an early event in the process of axonal degeneration. This effect suggests that MPP+ and 6-OHDA may act upon a common pathway and that this pathway is present in both DA and non-DA neurons. Previous reports using MPP+ showed increased movement speed of mitochondria in the retrograde direction post-toxin treatment. In this study, we noted that while 6-OHDA decreased the overall proportion of moving mitochondria, the speed of those that are still moving remain dramatically unchanged. The mechanism behind this

phenomenon is unclear. Many regulators of mitochondria movement remain unknown and of those that are known, it is not clear how they affect mitochondrial transport speed.

A model proposed by Youle suggests that the halting of mitochondrial movement is related to recruitment of Pink1 and Parkin (Narendra, Walker et al. 2012). Pink1 and Parkin are regulators of mitochondrial dynamics and morphology (Wang, Chou et al. 2011) and have been shown affect not only mitochondrial transport (Kane and Youle 2011), but also other aspects, such as removal and fusion/fission. It has been suggested that damage to mitochondrial membrane potential stops the quick turnover rate of Pink1 upon the mitochondrial membrane (Jin, Lazarou et al. 2010). Stabilization of Pink1 recruits and activates Parkin (Lazarou, Jin et al. 2012; Lazarou, Narendra et al. 2013), potentially by acting upon mitofusin2, which then recruits Parkin to the damaged organelle (Chen and Dorn 2013). Parkin is an E3 ligase and targets proteins of the mitochondria-motor adaptor complex, Miro (Wang, Winter et al. 2011) and Milton (Glauser, Sonnay et al. 2011), for removal. The ubiquitination and degradation of the Miro/Milton adaptor complex effectively detaches the mitochondria from the motor proteins and thus effectively halts and sequesters the damaged mitochondria (Wang, Winter et al. 2011). However, it is unclear what happens next to the stopped mitochondria. Does it remain at its location until mitophagy occurs and an autophagosome forms around the mitochondria? So are the mitochondria that are still moving actually contained within autophagosomes? It may be possible that an alternate adaptor-motor system is in place which could identify an immobile and damaged mitochondria and then move it towards the cell body for removal.

Unfortunately, the mechanism underlying axonal degeneration is unknown, but experimental evidence has suggested that it is a distinct process from programmed cell death. JNK2 have been shown to be essential for apoptosis as it can translocate to mitochondria and mediate the

release of cytochrome c. In JNK2 and 3 null mice models, apoptosis was completely abrogated, and there was increased survival of neuronal cell bodies despite treatment with 6-OHDA. However, it was noted that protection against apoptosis via this pathway did not extend to the axons(Ries, Silva et al. 2008). The WLDS mutant protein is able to significantly delay axonal degeneration caused by both physical axotomy and biochemical insults, such as MPP+ but has shown little capacity to rescue neuronal cell bodies.(Hasbani and O'Malley 2006; Coleman and Freeman 2010) How WLDS confer its protection is unclear, but it is interesting to note that the mitochondria of WLD(S)+ axons showed not only increased basal mitochondrial transport but also increased capacity to buffer Ca^{2+} ions (Avery, Rooney et al. 2012). In addition, Wld(S) has been shown to regulate release of calcium ions via the mitochondrial transition pore (Barrientos, Martinez et al. 2011). After axotomy, there is an increase in the levels of intracellular calcium ions. Typically these calcium ions would activate calcium dependent proteases, such as calpain and once activated, calpain may cleave neurofilaments and microtubule associated proteins, such as spectrin and tubulin (Billger, Wallin et al. 1988; Johnson, Litersky et al. 1991). In WLD(S) axons, the high burst of calcium influx was highly suppressed after axotomy perhaps due to the increased buffering provided by WLD(S) mitochondria(Avery, Rooney et al. 2012).

Interestingly, 6-OHDA also decreased the movement of synaptic vesicles in both DA and non-DA axons and not just mitochondria. Previously, it was observed that MPP+ decreased the movement of only mitochondria but not synaptic vesicles (Kim-Han, Antenor-Dorsey et al. 2011). The decrease in the movement of both mitochondria and vesicles suggests that 6-OHDA or the byproducts of its degradation may be potentially acting upon additional mechanisms of axonal transport, such as kinesin, dynein, or stress kinases (Falzone, Stokin et al. 2009). It has been found that hydrogen peroxide, one of the byproducts of 6-OHDA oxidation, decreases both mitochondrial motility and Golgi vesicle movement (Fang, Bourdette et al. 2012).

It has been controversial whether transport disruptions are due to mitochondrial dysfunction or some other factor such as microtubule destabilization/modification. Recently, it was shown that MPP+ affected microtubule post-translational modifications in a mouse *in vivo* model and that these modifications affect mitochondrial transport(Cartelli, Casagrande et al. 2013). However, that study did not show actual mitochondrial movement data and instead relied on the appearance of mitochondrial aggregates and axonal beading to demonstrate transport block. *In vitro*, mitochondrial movement decrease occurred prior to the appearance of axonal beading (Kim-Han, Antenor-Dorsey et al. 2011). The decrease in transport after exposure to 6-OHDA was not associated with mitochondrial fragmentation or loss of axonal integrity in this study or with hydrogen peroxide (Fang, Bourdette et al. 2012). Oxidative stress induced by hydrogen peroxide has led to increased

In vivo, injection of 6-OHDA into the striatum produced a progressive retrograde loss of DA axons, which subsequently resulted in heavy loss of DA cell bodies. Similarly, the results of this dissertation also show significant degeneration of DA cell bodies 48 hours after treatment with 6-OHDA and lend support to the theory of a dying back axonopathies. It was found that in the *in vivo* retrograde models of 6-OHDA-induced degeneration there were increased levels of autophagy, as marked by accumulation of LC3 and also DA degeneration (Cheng, Kim et al. 2011). In both MPP+(Kim-Han, Antenor-Dorsey et al. 2011) and 6-OHDA *in vitro* studies, smooth LC3-GFP labeling was seen along both the cell body and axons prior to toxin treatment. It was not until much later (3 hours for MPP+ and 9 hours for 6-OHDA) that there was punctated LC3-GFP labeling. Though co-labeling experiments would be useful in determining the localization and formation of autophagosomes around mitochondria and perhaps the degree of mitophagy, my data provides additional support to the idea that 6-OHDA can induce autophagy and that disruption to the autophagic system could play a role in leading to DA cell death(Dagda, Zhu et al. 2008; Li, Wang et al. 2011; Galindo, Solesio et al. 2012). The PI3K/AkT/mTOR pathway has been implicated in

maintaining DA axonal phenotype and axonal outgrowth (Kim, Chen et al. 2011; Kim, Ries et al. 2011). An active form of Akt offered protection against 6-OHDA induced axonal degeneration and significantly reduced LC3 punctas and autophagosome formation. In the same study, the authors also performed a conditional deletion of the protein Atg7, which is an essential mediator of autophagy, and found that this deletion limited the appearance of autophagosomes and protected against 6-OHDA induced axonal degeneration and (Cheng, Kim et al. 2011).

While subtle differences exist between the effects of two different toxins, MPP+ and 6-OHDA that cause parkinsonisms. It is clear that axonal transport disruptions play an early and important role in both models. With improper trafficking of mitochondria, there could be energy deficits and loss of function to various intra-axonal processes, which could eventually lead to axonal degeneration. Increased oxidative stress could stem from improper removal of mitochondria and lead to disruptions of other systems such as failure of ubiquitin-proteasome pathways and result in aggregation of misfolded proteins. As of right now, the details of an axonal degenerative pathway is unclear but the discovery of Sarm1, a protein required for the activation of injury-induced axonal degeneration points to the existence of an ancient and conserved axonal death signaling pathway(Osterloh, Yang et al. 2012). Whether this pathway could be targeted for the development of PD therapeutics or perhaps an axon regenerative pathway such as mTOR (Park, Liu et al. 2008; Park, Liu et al. 2010) could be used currently remains unknown. However, the development of microfluidic devices and genetic screens renders previously intractable problems solvable. These new technologies continue to enhance and expand the available toolset for understanding key biological processes in order to develop better therapies for patients suffering from major neurological disorders.

Chapter 4

Summary and Future Directions

4.1 Summary of findings

This dissertation demonstrated the design and construction of microfluidic devices for isolating and orienting axons, and then used these devices to study specific axonal transport processes in isolation from the dendrites and cell bodies. The goals of the dissertation were fulfilled by 1) identifying the design constraints for a microfluidic device that can support the culture of sensitive primary mesencephalic neurons, as well as conducting assays in isolated and aligned axons and 2) investigating the mechanisms and effect of 6-OHDA, a commonly used parkinsonism toxin, on aspects of axonal transport, such as mitochondrial movement and microtubule stability.

The first objective of the dissertation was to design a cellular compartment strategy that would allow for the culturing of sensitive primary midbrain neurons. Essential requirements included exposing the neurons to minimal stress during the plating process as well as subsequent feedings. The neurons also had to be plated as close to the entrances to the microchannels as possible so that they have the opportunity to find and extend their axons into the microchannels. They had to be exposed directly to a sufficient quantity of fresh media, and the strategy had to allow for direct access of toxins to the neurons so that the concentration of the toxin can be controlled.

So based on the previously listed requirements, it was hypothesized that an open compartment would fulfill all of these conditions rather than an enclosed compartment as seen in the Jeon microdevice(Taylor, Rhee et al. 2003; Lu, Kim-Han et al. 2012). It has already been shown

that primary neurons can survive in the open well environment of compartmented devices previously made by Ivins (Ivins, Bui et al. 1998). Ivin's device was composed of two large semi-circular Teflon pieces with a glass slide acting as a partition for dividing the somal and axonal compartment. It was reasonable to hypothesize that the DA neurons may also survive within the same geometric considerations of an open compartmented device made using PDMS. Another important consideration for the design of the microdevice is the geometry of the microchannels. For these experiments, both 10 and 5 μm width microchannels were used. The 5 μm width seemed to provide higher number of single axons available for study compared to the 10 μm channels where axonal bundling was more common. Peyrin had performed a study looking at the effects of different channel width upon the number and health of axons within each channel(Peyrin, Deleglise et al. 2011). They had found channel sizes below 3 μm led to unhealthy axons where as channel sizes above 10 μm led to even more axonal bundling.

The second part of the dissertation was to use the microdevice to study the effects that 6-OHDA had on different aspects of axonal transport within dopaminergic neurons. It was found that 6-OHDA quickly depolarized mitochondrial membranes and led to a decrease in the fraction of motile mitochondria within 30 minutes. Of the mitochondria that were still motile, there did not seem to have been an effect upon the velocity of the mitochondria nor was there increased mitochondrial transport in the retrograde direction as was previously observed with MPP+. The decrease in mitochondrial motility was seen in both dopaminergic and non-dopaminergic neurons. 6-OHDA also affected the movement of synaptic vesicles, decreasing their motility in both anterograde and retrograde directions. No changes to the size of the mitochondria were observed between control and 6-OHDA-treated groups at 30 minutes. Microtubule fragmentation did not occur until after 6 hours of treatment with 6-OHDA and could be due to mitochondrial dysfunction. Treatment with 6-OHDA in the axonal chamber led to a retrograde degenerative

model of cellular degeneration similar to what was seen *in vivo* as a significant amount of cell death occurred after 48 hours. Previously, NAC, a glutathione precursor and MnTBAP, a cell-permeant SOD1 mimetic, were able to protect axons and cell bodies from the effects of 6-OHDA. In these experiments, they were also able to prevent the loss of mitochondrial movement after 6-OHDA exposure. However, EGTA, a calcium ion chelator, did not offer protection against 6-OHDA's effects on mitochondrial transport. This second part of the dissertation therefore suggests that 6-OHDA's toxicity is due to the generation of high levels of ROS, which increases oxidative stress within the cell. This study also suggests the importance of transport dysfunction as an initial event in the onset of axonal injury and may play a role in leading the cascade of events that leads to failure.

The conclusions derived from the results of the dissertation suggest the usefulness of microfluidic devices in helping to answer many fundamental questions of biology and the underlying axonal degenerative mechanisms into neurodegenerative diseases.

4.2 Recommendations for Future Directions

While this dissertation work has achieved the development of a tool to answer some of the questions regarding what happens to axonal transport processes when a neurodegenerative toxin is introduced, many biological questions remain unanswered, not only about the mechanisms involved in the dying-back process of PD but also many other neurodegenerative diseases as well.

4.2.1. Unidirectional three compartmented microdevices.

Considering the potential application of the microdevice for the study of neuronal networks using co-cultures of different neuronal populations, the symmetrical nature of the microchannels currently used are not ideal as both neuronal populations may extend axons into the microchannels and synapse on to each one another. It would be desirable to have unidirectional signaling to better recapitulate what is observed *in vivo* in which one neuron subtype would synapse onto another and not vice versa. Peyrin developed an axon diode concept in which an asymmetrical funnel shaped microchannel would prevent neurite extensions from one group of cells and permit extensions from another(Peyrin, Deleglise et al. 2011). Using this axon diode concept and the open compartment chamber, one can design a compartment (fig 5.1) to model the network of dopaminergic, striatal, and cortical neurons and then study the propagation of disease pathology through this network. Striatal neurons that are part of the nigrostriatal pathway receive both DA and cortical innervation. However, striatal neurons do not synapse onto DA or cortical neurons. Loss of cortical neurons contributes to the progression of dementia in PD patients (Dauer and Przedborski 2003). Given the preponderance of evidence pointing to axonal and cellular degeneration beginning within areas of the striatum, it would be interesting to model and study network behavior and the spread of degenerative behavior within this network. Experiments can be done to investigate the impact of PD toxins MPP+ and 6-OHDA or genetic models of PD, such as the use of mutated α-synuclein fibrils (Volpicelli-Daley, Luk et al. 2011) on the network. Using the axon diode concept, dopaminergic and cortical innervation of striatal culture could be achieved without the possibility of cross contamination (Fig. 4.1).

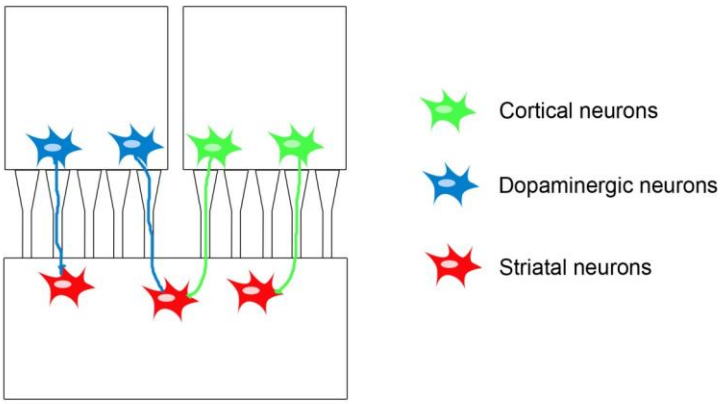

.

Figure 4.1 Schematic for three chambered unidirectional microdevice: Different neuronal populations could be loaded in three compartments connected by asymmetrical microchannels. This asymmetry supports unidirectional synapse formation where cortical/DA neurons can synapse onto striatal neurons but not vice versa.

4.2.2 Wells for high throughput imaging

Since axonal degeneration appear early in the development of multiple major neurodegenerative diseases (Coleman 2005), development of future therapies should be targeted towards maintaining the health and function of axons (Burke and O'Malley 2012). Drug treatments to maintain the survivability of cell body may be too little and too late in stopping the progression of these disorders. However, the drug screening process is logistically difficult given the lack of compartmentalization to achieve axonal separation with current high-throughput methods, such as the use of 96 well plates. The density and health of axons would obviously be the metric of drug efficacy. Existing compartmented chambers, such as the Campenot or microfluidic devices can only be used to screen a few toxins at a time. However, the problem of high-throughput axonal imaging could be overcome with miniaturization and rapid prototyping. While PDMS is the go to material for developing microfluidic devices, polystyrene is another material which can be easily molded and

adapted to creating compartmented chambers. Incorporation of a thin divider into each well of a 96 well polystyrene plate could potentially create a compartmented chamber within each well (Fig. 4.2). Having the divider span the diameter of the well and creating a small and wide tunnel through which neurites could extend would effectively separate the axons from the dendrites and cell bodies similar to what was achieved in Ivin's compartmented device (Ivins, Bui et al. 1998). Each well could then be used to screen for a different compound to assess their effectiveness in preservation of axonal integrity in a toxin model.

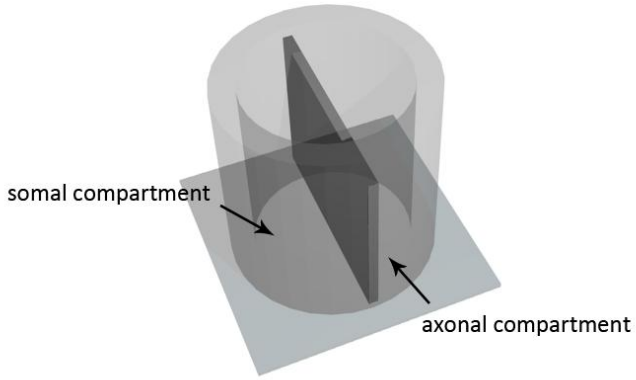

Figure 4.2 Schematic for 96 well plate compartments. Compartmented 96 well plates could be modified for high throughput screening of axon protective compounds.

4.3 Future work for understanding the mechanisms of PD

4.3.1 6-OHDA and Parkin.

From the second aim of this dissertation, it was observed that 6-OHDA quickly depolarizes mitochondria. Current model suggests that Pink1 accumulation on the depolarized mitochondria's

membrane surface would recruit Parkin which then leads to the degradation of adaptor proteins and disconnect the mitochondria from motor protein (Wang, Winter et al. 2011). However, whether this model is true for all cases remains to be seen. Unpublished observations using CCCP to decouple mitochondria electron transport chain rapidly led to the depolarization of mitochondria within 10 minutes. However, at this stage most of the mitochondria were still moving. Parkin was not yet recruited to the mitochondria at this time. This suggests that mitochondria depolarization may not necessarily recruit Parkin and this difference may depend upon the cell type. Whether 6-OHDA induces Parkin localization to depolarized mitochondria would be important to addressing the validity of the model.

4.3.2 Wld(S) and Mitochondrial transport

It was found that Wld(S) significantly delayed axonal degeneration in physical axotomy (Coleman and Freeman 2010) and also PD toxins, MPP+ and 6-OHDA model (Cheng and Burke 2010; Antenor-Dorsey and O'Malley 2012). However, an interesting observation was made by the Burke group in an in vivo model of 6-OHDA. They found that Wld(S) delayed anterograde axonal degeneration but surprisingly had no effect on retrograde 6-OHDA induced degeneration (Cheng and Burke 2010). This difference suggests that anterograde and retrograde axonal degeneration may be mediated by different pathways. By using the fluidic isolation offered by the microchannels, it would be simple to culture a set of Wld(S)+ neurons in the somal compartment and then establish an in vitro model of anterograde and retrograde axonal degeneration induced by 6-OHDA. Various aspects of axonal transport processes, such as mitochondrial movement, the axonal localization of the Wld(S) protein, and calcium properties of the midbrain neurons could then be studied under both anterograde and retrograde degenerative models.

4.4 Concluding Remarks

The overall intention of this dissertation was to develop a microfluidic device capable of isolating and studying axonal transport processes within mesencephalic axons. Disruptions to axonal transport and also axonal degeneration are early events in the etiology of neurodegenerative diseases, such as PD and Huntington's' disease. Understanding how axonal transport occurs as well as what pathways are involved in the maintenance of axonal structure and function, could lead to the development of better therapies for curing neurodegenerative diseases that may have multiple causes but whose causes converge on a single pathway.

References

Antenor-Dorsey, J. A. and K. L. O'Malley (2012). "WldS but not Nmnat1 protects dopaminergic neurites from MPP+ neurotoxicity." Mol Neurodegener **7**: 5.

Araki, T., Y. Sasaki, et al. (2004). "Increased nuclear NAD biosynthesis and SIRT1 activation prevent axonal degeneration." Science **305**(5686): 1010-1013.

Avery, M. A., T. M. Rooney, et al. (2012). "WldS prevents axon degeneration through increased mitochondrial flux and enhanced mitochondrial Ca2+ buffering." Curr Biol **22**(7): 596-600.

Barrientos, S. A., N. W. Martinez, et al. (2011). "Axonal degeneration is mediated by the mitochondrial permeability transition pore." J Neurosci **31**(3): 966-978.

Beaudet, A. L. and J. W. Belmont (2008). "Array-Based DNA Diagnostics: Let the Revolution Begin." Annual Review of Medicine **59**(1): 113-129.

Ben-Yakar, A., N. Chronis, et al. (2009). "Microfluidics for the analysis of behavior, nerve regeneration, and neural cell biology in C. elegans." Curr Opin Neurobiol **19**(5): 561-567.

Berdichevsky, Y., H. Sabolek, et al. (2009). "Microfluidics and multielectrode array-compatible organotypic slice culture method." J Neurosci Methods **178**(1): 59-64.

Bernheimer, H., W. Birkmayer, et al. (1973). "Brain dopamine and the syndromes of Parkinson and Huntington. Clinical, morphological and neurochemical correlations." J Neurol Sci **20**(4): 415-455.

Bernstein, A. I., S. P. Garrison, et al. (2011). "6-OHDA generated ROS induces DNA damage and p53- and PUMA-dependent cell death." Mol Neurodegener **6**(1): 2.

Berthier, E., E. W. Young, et al. (2012). "Engineers are from PDMS-land, Biologists are from Polystyrenia." Lab Chip **12**(7): 1224-1237.

Betarbet, R., T. B. Sherer, et al. (2000). "Chronic systemic pesticide exposure reproduces features of Parkinson's disease." Nat Neurosci **3**(12): 1301-1306.

Bhattacharjee, N., N. Li, et al. (2010). "A neuron-benign microfluidic gradient generator for studying the response of mammalian neurons towards axon guidance factors." Integr Biol (Camb) **2**(11-12): 669-679.

Billger, M., M. Wallin, et al. (1988). "Proteolysis of tubulin and microtubule-associated proteins 1 and 2 by calpain I and II. Difference in sensitivity of assembled and disassembled microtubules." Cell Calcium **9**(1): 33-44.

Blum, D., S. Torch, et al. (2001). "Molecular pathways involved in the neurotoxicity of 6-OHDA, dopamine and MPTP: contribution to the apoptotic theory in Parkinson's disease." Prog Neurobiol **65**(2): 135-172.

Blum, D., S. Torch, et al. (2000). "Extracellular toxicity of 6-hydroxydopamine on PC12 cells." Neurosci Lett **283**(3): 193-196.

Bonifati, V., P. Rizzu, et al. (2003). "DJ-1(PARK7), a novel gene for autosomal recessive, early onset parkinsonism." Neurol Sci **24**(3): 159-160.

Breese, G. R. and T. D. Traylor (1970). "Effect of 6-hydroxydopamine on brain norepinephrine and dopamine evidence for selective degeneration of catecholamine neurons." J Pharmacol Exp Ther **174**(3): 413-420.

Bryzek, J., K. Peterson, et al. (1994). "Micromachines on the march." Spectrum, IEEE **31**(5): 20-31.

Burke, R. E. and K. O'Malley (2012). "Axon degeneration in Parkinson's disease." Exp Neurol.

Campenot, R. B. (1977). "Local control of neurite development by nerve growth factor." Proc Natl Acad Sci U S A **74**(10): 4516-4519.

Campenot, R. B. (1982). "Development of sympathetic neurons in compartmentalized cultures. II. Local control of neurite survival by nerve growth factor." Dev Biol **93**(1): 13-21.

Campenot, R. B. (1987). "Local control of neurite sprouting in cultured sympathetic neurons by nerve growth factor." Brain Res **465**(1-2): 293-301.
Candy, J. M., R. H. Perry, et al. (1983). "Pathological changes in the nucleus of Meynert in Alzheimer's and Parkinson's diseases." J Neurol Sci **59**(2): 277-289.
Cappelletti, G., B. Pedrotti, et al. (2001). "Microtubule assembly is directly affected by MPP(+)in vitro." Cell Biol Int **25**(10): 981-984.
Cappelletti, G., T. Surrey, et al. (2005). "The parkinsonism producing neurotoxin MPP+ affects microtubule dynamics by acting as a destabilising factor." FEBS Lett **579**(21): 4781-4786.
Cartelli, D., F. Casagrande, et al. (2013). "Microtubule alterations occur early in experimental parkinsonism and the microtubule stabilizer epothilone d is neuroprotective." Sci Rep **3**: 1837.
Cartelli, D., S. Goldwurm, et al. (2012). "Microtubule destabilization is shared by genetic and idiopathic Parkinson's disease patient fibroblasts." PLoS One **7**(5): e37467.
Cartelli, D., C. Ronchi, et al. (2010). "Microtubule dysfunction precedes transport impairment and mitochondria damage in MPP+ -induced neurodegeneration." J Neurochem **115**(1): 247-258.
Charcot, J. M. and Bourneville (1872). Leçons sur les maladies du système nerveux faites à la salpêtrière. Paris, A. Delahaye.
Chen, Y. and G. W. Dorn, 2nd (2013). "PINK1-phosphorylated mitofusin 2 is a Parkin receptor for culling damaged mitochondria." Science **340**(6131): 471-475.
Cheng, H. C. and R. E. Burke (2010). "The Wld(S) mutation delays anterograde, but not retrograde, axonal degeneration of the dopaminergic nigro-striatal pathway in vivo." J Neurochem **113**(3): 683-691.
Cheng, H. C., S. R. Kim, et al. (2011). "Akt suppresses retrograde degeneration of dopaminergic axons by inhibition of macroautophagy." J Neurosci **31**(6): 2125-2135.
Cheng, H. C., C. M. Ulane, et al. (2010). "Clinical progression in Parkinson disease and the neurobiology of axons." Ann Neurol **67**(6): 715-725.
Choi, W. S., L. M. Canzoniero, et al. (1999). "Characterization of MPP(+)-induced cell death in a dopaminergic neuronal cell line: role of macromolecule synthesis, cytosolic calcium, caspase, and Bcl-2-related proteins." Exp Neurol **159**(1): 274-282.
Choi, W. S., R. D. Palmiter, et al. (2011). "Loss of mitochondrial complex I activity potentiates dopamine neuron death induced by microtubule dysfunction in a Parkinson's disease model." J Cell Biol **192**(5): 873-882.
Choi, W. S., S. Y. Yoon, et al. (1999). "Two distinct mechanisms are involved in 6-hydroxydopamine- and MPP+-induced dopaminergic neuronal cell death: role of caspases, ROS, and JNK." J Neurosci Res **57**(1): 86-94.
Chu, Y., G. A. Morfini, et al. (2012). "Alterations in axonal transport motor proteins in sporadic and experimental Parkinson's disease." Brain **135**(Pt 7): 2058-2073.
Chung, K., M. Crane, et al. (2009). "Automated on-chip imaging and sorting of C. elegans."
Clarson, S. J. and J. A. Semlyen (1993). Siloxane polymers. Englewood Cliffs, N.J., Prentice Hall.
Cleeter, M. W., J. M. Cooper, et al. (1992). "Irreversible inhibition of mitochondrial complex I by 1-methyl-4-phenylpyridinium: evidence for free radical involvement." J Neurochem **58**(2): 786-789.
Clement, M. V., L. H. Long, et al. (2002). "The cytotoxicity of dopamine may be an artefact of cell culture." J Neurochem **81**(3): 414-421.
Coleman, M. (2005). "Axon degeneration mechanisms: commonality amid diversity." Nat Rev Neurosci **6**(11): 889-898.
Coleman, M. P. and M. R. Freeman (2010). "Wallerian degeneration, wld(s), and nmnat." Annu Rev Neurosci **33**: 245-267.

Corti, O., S. Lesage, et al. (2011). "What genetics tells us about the causes and mechanisms of Parkinson's disease." Physiol Rev **91**(4): 1161-1218.
Curtius, H. C., M. Wolfensberger, et al. (1974). "Mass fragmentography of dopamine and 6-hydroxydopamine. Application to the determination of dopamine in human brain biopsies from the caudate nucleus." J Chromatogr **99**(0): 529-540.
Dagda, R. K., S. J. Cherra, 3rd, et al. (2009). "Loss of PINK1 function promotes mitophagy through effects on oxidative stress and mitochondrial fission." J Biol Chem **284**(20): 13843-13855.
Dagda, R. K., J. Zhu, et al. (2008). "Mitochondrially localized ERK2 regulates mitophagy and autophagic cell stress: implications for Parkinson's disease." Autophagy **4**(6): 770-782.
Dauer, W. and S. Przedborski (2003). "Parkinson's disease: mechanisms and models." Neuron **39**(6): 889-909.
Davis, G. C., A. C. Williams, et al. (1979). "Chronic Parkinsonism secondary to intravenous injection of meperidine analogues." Psychiatry Res **1**(3): 249-254.
Davison, A. J., N. A. Legault, et al. (1986). "Effect of 6-hydroxydopamine on polymerization of tubulin. Protection by superoxide dismutase, catalase, or anaerobic conditions." Biochem Pharmacol **35**(9): 1411-1417.
Driver, J. A., G. Logroscino, et al. (2009). "Incidence and remaining lifetime risk of Parkinson disease in advanced age." Neurology **72**(5): 432-438.
Ehringer, H. and O. Hornykiewicz (1960). "[Distribution of noradrenaline and dopamine (3-hydroxytyramine) in the human brain and their behavior in diseases of the extrapyramidal system]." Klin Wochenschr **38**: 1236-1239.
Falzone, T. L., G. B. Stokin, et al. (2009). "Axonal stress kinase activation and tau misbehavior induced by kinesin-1 transport defects." J Neurosci **29**(18): 5758-5767.
Fang, C., D. Bourdette, et al. (2012). "Oxidative stress inhibits axonal transport: implications for neurodegenerative diseases." Mol Neurodegener **7**: 29.
Fearnley, J. M. and A. J. Lees (1991). "Ageing and Parkinson's disease: substantia nigra regional selectivity." Brain **114 (Pt 5)**: 2283-2301.
Finn, J. T., M. Weil, et al. (2000). "Evidence that Wallerian degeneration and localized axon degeneration induced by local neurotrophin deprivation do not involve caspases." J Neurosci **20**(4): 1333-1341.
Forno, L. S., L. E. DeLanney, et al. (1993). "Similarities and differences between MPTP-induced parkinsonsim and Parkinson's disease. Neuropathologic considerations." Adv Neurol **60**: 600-608.
Forno, L. S., J. W. Langston, et al. (1986). "Locus ceruleus lesions and eosinophilic inclusions in MPTP-treated monkeys." Ann Neurol **20**(4): 449-455.
Fransson, S., A. Ruusala, et al. (2006). "The atypical Rho GTPases Miro-1 and Miro-2 have essential roles in mitochondrial trafficking." Biochem Biophys Res Commun **344**(2): 500-510.
Fuller, R. W. and S. K. Hemrick-Luecke (1985). "Effects of amfonelic acid, alpha-methyltyrosine, Ro 4-1284 and haloperidol pretreatment on the depletion of striatal dopamine by 1-methyl-4-phenyl-1,2,3,6-tetrahydropyridine in mice." Res Commun Chem Pathol Pharmacol **48**(1): 17-25.
Galindo, M. F., M. E. Solesio, et al. (2012). "Mitochondrial dynamics and mitophagy in the 6-hydroxydopamine preclinical model of Parkinson's disease." Parkinsons Dis **2012**: 131058.
Geppert, L. (1996). "Semiconductor lithography for the next millennium." Spectrum, IEEE **33**(4): 33-38.
Gispert, S., F. Ricciardi, et al. (2009). "Parkinson phenotype in aged PINK1-deficient mice is accompanied by progressive mitochondrial dysfunction in absence of neurodegeneration." PLoS One **4**(6): e5777.
Glater, E. E., L. J. Megeath, et al. (2006). "Axonal transport of mitochondria requires milton to recruit kinesin heavy chain and is light chain independent." J Cell Biol **173**(4): 545-557.

Glauser, L., S. Sonnay, et al. (2011). "Parkin promotes the ubiquitination and degradation of the mitochondrial fusion factor mitofusin 1." J Neurochem **118**(4): 636-645.
Glinka, Y. Y. and M. B. Youdim (1995). "Inhibition of mitochondrial complexes I and IV by 6-hydroxydopamine." Eur J Pharmacol **292**(3-4): 329-332.
Goldberg, M. S., S. M. Fleming, et al. (2003). "Parkin-deficient mice exhibit nigrostriatal deficits but not loss of dopaminergic neurons." J Biol Chem **278**(44): 43628-43635.
Greenfield, J. G. and F. D. Bosanquet (1953). "The brain-stem lesions in Parkinsonism." J Neurol Neurosurg Psychiatry **16**(4): 213-226.
Haas, R. H., F. Nasirian, et al. (1995). "Low platelet mitochondrial complex I and complex II/III activity in early untreated Parkinson's disease." Ann Neurol **37**(6): 714-722.
Hanrott, K., L. Gudmunsen, et al. (2006). "6-hydroxydopamine-induced apoptosis is mediated via extracellular auto-oxidation and caspase 3-dependent activation of protein kinase Cdelta." J Biol Chem **281**(9): 5373-5382.
Hasbani, D. M. and K. L. O'Malley (2006). "Wld(S) mice are protected against the Parkinsonian mimetic MPTP." Exp Neurol **202**(1): 93-99.
Heeman, B., C. Van den Haute, et al. (2011). "Depletion of PINK1 affects mitochondrial metabolism, calcium homeostasis and energy maintenance." J Cell Sci **124**(Pt 7): 1115-1125.
Herkenham, M., M. D. Little, et al. (1991). "Selective retention of MPP+ within the monoaminergic systems of the primate brain following MPTP administration: an in vivo autoradiographic study." Neuroscience **40**(1): 133-158.
Holtz, W. A. and K. L. O'Malley (2003). "Parkinsonian mimetics induce aspects of unfolded protein response in death of dopaminergic neurons." J Biol Chem **278**(21): 19367-19377.
Holtz, W. A., J. M. Turetzky, et al. (2006). "Oxidative stress-triggered unfolded protein response is upstream of intrinsic cell death evoked by parkinsonian mimetics." J Neurochem **99**(1): 54-69.
Holtz, W. A., J. M. Turetzky, et al. (2005). "Microarray expression profiling identifies early signaling transcripts associated with 6-OHDA-induced dopaminergic cell death." Antioxid Redox Signal **7**(5-6): 639-648.
Hornykiewicz, O. (1998). "Biochemical aspects of Parkinson's disease." Neurology **51**(2 Suppl 2): S2-9.
Hur, E. M., I. H. Yang, et al. (2011). "Engineering neuronal growth cones to promote axon regeneration over inhibitory molecules." Proc Natl Acad Sci U S A **108**(12): 5057-5062.
Iglesias-Gonzalez, J., S. Sanchez-Iglesias, et al. (2012). "Differential toxicity of 6-hydroxydopamine in SH-SY5Y human neuroblastoma cells and rat brain mitochondria: protective role of catalase and superoxide dismutase." Neurochem Res **37**(10): 2150-2160.
Ivins, K. J., E. T. Bui, et al. (1998). "Beta-amyloid induces local neurite degeneration in cultured hippocampal neurons: evidence for neuritic apoptosis." Neurobiol Dis **5**(5): 365-378.
Jin, S. M., M. Lazarou, et al. (2010). "Mitochondrial membrane potential regulates PINK1 import and proteolytic destabilization by PARL." J Cell Biol **191**(5): 933-942.
Johnson, G. V., J. M. Litersky, et al. (1991). "Degradation of microtubule-associated protein 2 and brain spectrin by calpain: a comparative study." J Neurochem **56**(5): 1630-1638.
Jokinen, V., P. Sakha, et al. (2013). "A microfluidic chip for axonal isolation and electrophysiological measurements." J Neurosci Methods **212**(2): 276-282.
Kane, L. A. and R. J. Youle (2011). "PINK1 and Parkin flag Miro to direct mitochondrial traffic." Cell **147**(4): 721-723.
Kim-Han, J. S., J. A. Antenor-Dorsey, et al. (2011). "The parkinsonian mimetic, MPP+, specifically impairs mitochondrial transport in dopamine axons." J Neurosci **31**(19): 7212-7221.
Kim, H. J., J. W. Park, et al. (2012). "Quantitative Analysis of Axonal Transport by Using Compartmentalized and Surface Micropatterned Culture of Neurons." ACS Chemical Neuroscience **3**(6): 433-438.

Kim, S. R., X. Chen, et al. (2011). "Dopaminergic pathway reconstruction by Akt/Rheb-induced axon regeneration." Ann Neurol **70**(1): 110-120.
Kim, S. R., V. Ries, et al. (2011). "Age and alpha-synuclein expression interact to reveal a dependence of dopaminergic axons on endogenous Akt/PKB signaling." Neurobiol Dis **44**(2): 215-222.
Kim, Y. T., K. Karthikeyan, et al. (2009). "Neuro-optical microfluidic platform to study injury and regeneration of single axons." Lab Chip **9**(17): 2576-2581.
Kirik, D., B. Georgievska, et al. (2004). "Localized striatal delivery of GDNF as a treatment for Parkinson disease." Nat Neurosci **7**(2): 105-110.
Kitada, T., S. Asakawa, et al. (1998). "Mutations in the parkin gene cause autosomal recessive juvenile parkinsonism." Nature **392**(6676): 605-608.
Kitada, T., Y. Tong, et al. (2009). "Absence of nigral degeneration in aged parkin/DJ-1/PINK1 triple knockout mice." J Neurochem **111**(3): 696-702.
Kramer, M. L. and W. J. Schulz-Schaeffer (2007). "Presynaptic alpha-synuclein aggregates, not Lewy bodies, cause neurodegeneration in dementia with Lewy bodies." J Neurosci **27**(6): 1405-1410.
Kulich, S. M. and C. T. Chu (2003). "Role of reactive oxygen species in extracellular signal-regulated protein kinase phosphorylation and 6-hydroxydopamine cytotoxicity." J Biosci **28**(1): 83-89.
Kuma, A., M. Matsui, et al. (2007). "LC3, an autophagosome marker, can be incorporated into protein aggregates independent of autophagy: caution in the interpretation of LC3 localization." Autophagy **3**(4): 323-328.
Kunze, A., R. Meissner, et al. (2011). "Co-pathological connected primary neurons in a microfluidic device for Alzheimer studies." Biotechnol Bioeng **108**(9): 2241-2245.
Langston, J. W., P. Ballard, et al. (1983). "Chronic Parkinsonism in humans due to a product of meperidine-analog synthesis." Science **219**(4587): 979-980.
Lazarou, M., S. M. Jin, et al. (2012). "Role of PINK1 binding to the TOM complex and alternate intracellular membranes in recruitment and activation of the E3 ligase Parkin." Dev Cell **22**(2): 320-333.
Lazarou, M., D. P. Narendra, et al. (2013). "PINK1 drives Parkin self-association and HECT-like E3 activity upstream of mitochondrial binding." J Cell Biol **200**(2): 163-172.
Lee, C. S., A. Samii, et al. (2000). "In vivo positron emission tomographic evidence for compensatory changes in presynaptic dopaminergic nerve terminals in Parkinson's disease." Ann Neurol **47**(4): 493-503.
Lees, A. J., J. Hardy, et al. (2009). "Parkinson's disease." Lancet **373**(9680): 2055-2066.
Li, L., X. Wang, et al. (2011). "Parkinson's disease involves autophagy and abnormal distribution of cathepsin L." Neurosci Lett **489**(1): 62-67.
Li, Y., W. Liu, et al. (2009). "Mutant LRRK2(R1441G) BAC transgenic mice recapitulate cardinal features of Parkinson's disease." Nat Neurosci **12**(7): 826-828.
Liu, W., R. Acin-Perez, et al. (2011). "Pink1 regulates the oxidative phosphorylation machinery via mitochondrial fission." Proc Natl Acad Sci U S A **108**(31): 12920-12924.
Liu, W. W., J. Goodhouse, et al. (2008). "A microfluidic chamber for analysis of neuron-to-cell spread and axonal transport of an alpha-herpesvirus." PLoS One **3**(6): e2382.
Lotharius, J., L. L. Dugan, et al. (1999). "Distinct mechanisms underlie neurotoxin-mediated cell death in cultured dopaminergic neurons." J Neurosci **19**(4): 1284-1293.
Lotharius, J. and K. L. O'Malley (2000). "The parkinsonism-inducing drug 1-methyl-4-phenylpyridinium triggers intracellular dopamine oxidation. A novel mechanism of toxicity." J Biol Chem **275**(49): 38581-38588.
Lu, X., J. S. Kim-Han, et al. (2012). "A microdevice platform for visualizing mitochondrial transport in aligned dopaminergic axons." J Neurosci Methods **209**(1): 35-39.

Lunn, E. R., V. H. Perry, et al. (1989). "Absence of Wallerian Degeneration does not Hinder Regeneration in Peripheral Nerve." Eur J Neurosci **1**(1): 27-33.
Luthman, J., A. Fredriksson, et al. (1989). "Selective lesion of central dopamine or noradrenaline neuron systems in the neonatal rat: motor behavior and monoamine alterations at adult stage." Behav Brain Res **33**(3): 267-277.
Majumdar, D., Y. Gao, et al. (2011). "Co-culture of neurons and glia in a novel microfluidic platform." J Neurosci Methods **196**(1): 38-44.
Markey, S. P., J. N. Johannessen, et al. (1984). "Intraneuronal generation of a pyridinium metabolite may cause drug-induced parkinsonism." Nature **311**(5985): 464-467.
Maroteaux, L., J. T. Campanelli, et al. (1988). "Synuclein: a neuron-specific protein localized to the nucleus and presynaptic nerve terminal." J Neurosci **8**(8): 2804-2815.
Marti, M. J., J. Saura, et al. (2002). "Striatal 6-hydroxydopamine induces apoptosis of nigral neurons in the adult rat." Brain Res **958**(1): 185-191.
Martin, M., S. J. Iyadurai, et al. (1999). "Cytoplasmic dynein, the dynactin complex, and kinesin are interdependent and essential for fast axonal transport." Mol Biol Cell **10**(11): 3717-3728.
Mayeux, R. (2003). "Epidemiology of neurodegeneration." Annu Rev Neurosci **26**: 81-104.
Meissner, W., C. Prunier, et al. (2003). "Time-course of nigrostriatal degeneration in a progressive MPTP-lesioned macaque model of Parkinson's disease." Mol Neurobiol **28**(3): 209-218.
Mijatovic, J., M. Piltonen, et al. (2011). "Constitutive Ret signaling is protective for dopaminergic cell bodies but not for axonal terminals." Neurobiol Aging **32**(8): 1486-1494.
Misko, A., S. Jiang, et al. (2010). "Mitofusin 2 is necessary for transport of axonal mitochondria and interacts with the Miro/Milton complex." J Neurosci **30**(12): 4232-4240.
Mizushima, N. and M. Komatsu (2011). "Autophagy: renovation of cells and tissues." Cell **147**(4): 728-741.
Monteiro, H. P. and C. C. Winterbourn (1989). "6-Hydroxydopamine releases iron from ferritin and promotes ferritin-dependent lipid peroxidation." Biochem Pharmacol **38**(23): 4177-4182.
Morfini, G., G. Pigino, et al. (2007). "1-Methyl-4-phenylpyridinium affects fast axonal transport by activation of caspase and protein kinase C." Proc Natl Acad Sci U S A **104**(7): 2442-2447.
Nandhagopal, R., M. J. McKeown, et al. (2008). "Functional imaging in Parkinson disease." Neurology **70**(16 Pt 2): 1478-1488.
Narendra, D., A. Tanaka, et al. (2008). "Parkin is recruited selectively to impaired mitochondria and promotes their autophagy." J Cell Biol **183**(5): 795-803.
Narendra, D., J. E. Walker, et al. (2012). "Mitochondrial quality control mediated by PINK1 and Parkin: links to parkinsonism." Cold Spring Harb Perspect Biol **4**(11).
Narendra, D. P., S. M. Jin, et al. (2010). "PINK1 is selectively stabilized on impaired mitochondria to activate Parkin." PLoS Biol **8**(1): e1000298.
Nilsson, M. H., M. Patel, et al. (2013). "Subthalamic deep brain stimulation improves smooth pursuit and saccade performance in patients with Parkinson's disease." J Neuroeng Rehabil **10**: 33.
O'Malley, K. L. (2010). "The role of axonopathy in Parkinson's disease." Exp Neurobiol **19**(3): 115-119.
O'Malley, K. L., J. Liu, et al. (2003). "Targeted expression of BCL-2 attenuates MPP+ but not 6-OHDA induced cell death in dopaminergic neurons." Neurobiol Dis **14**(1): 43-51.
Olanow, C. W., Y. Agid, et al. (2004). "Levodopa in the treatment of Parkinson's disease: current controversies." Mov Disord **19**(9): 997-1005.
Olanow, C. W., M. B. Stern, et al. (2009). "The scientific and clinical basis for the treatment of Parkinson disease (2009)." Neurology **72**(21 Suppl 4): S1-136.
Orimo, S., T. Uchihara, et al. (2008). "Axonal alpha-synuclein aggregates herald centripetal degeneration of cardiac sympathetic nerve in Parkinson's disease." Brain **131**(Pt 3): 642-650.

Osterloh, J. M., J. Yang, et al. (2012). "dSarm/Sarm1 is required for activation of an injury-induced axon death pathway." Science **337**(6093): 481-484.
Palacino, J. J., D. Sagi, et al. (2004). "Mitochondrial dysfunction and oxidative damage in parkin-deficient mice." J Biol Chem **279**(18): 18614-18622.
Park, J., H. Koito, et al. (2009). "Microfluidic compartmentalized co-culture platform for CNS axon myelination research." Biomedical Microdevices **11**(6): 1145-1153.
Park, K. K., K. Liu, et al. (2010). "PTEN/mTOR and axon regeneration." Exp Neurol **223**(1): 45-50.
Park, K. K., K. Liu, et al. (2008). "Promoting axon regeneration in the adult CNS by modulation of the PTEN/mTOR pathway." Science **322**(5903): 963-966.
Parkinson, J. (1817). An essay on the shaking palsy, Printed by Whittingham and Rowland for Sherwood, Neely, and Jones.
Peyrin, J. M., B. Deleglise, et al. (2011). "Axon diodes for the reconstruction of oriented neuronal networks in microfluidic chambers." Lab Chip **11**(21): 3663-3673.
Pilling, A. D., D. Horiuchi, et al. (2006). "Kinesin-1 and Dynein are the primary motors for fast transport of mitochondria in Drosophila motor axons." Mol Biol Cell **17**(4): 2057-2068.
Polymeropoulos, M. H., C. Lavedan, et al. (1997). "Mutation in the alpha-synuclein gene identified in families with Parkinson's disease." Science **276**(5321): 2045-2047.
Poole, A. C., R. E. Thomas, et al. (2010). "The mitochondrial fusion-promoting factor mitofusin is a substrate of the PINK1/parkin pathway." PLoS One **5**(4): e10054.
Qin, D., Y. Xia, et al. (2010). "Soft lithography for micro- and nanoscale patterning." Nat Protoc **5**(3): 491-502.
Raff, M. C., A. V. Whitmore, et al. (2002). "Axonal self-destruction and neurodegeneration." Science **296**(5569): 868-871.
Rai-Choudhury, P. (1997). Handbook of microlithography, micromachining, and microfabrication. Bellingham, Wash., USA

London, UK, SPIE Optical Engineering Press ;

Institution of Electrical Engineers.
Ramsay, R. R. and T. P. Singer (1986). "Energy-dependent uptake of N-methyl-4-phenylpyridinium, the neurotoxic metabolite of 1-methyl-4-phenyl-1,2,3,6-tetrahydropyridine, by mitochondria." J Biol Chem **261**(17): 7585-7587.
Redman, P. T., B. S. Jefferson, et al. (2006). "A vital role for voltage-dependent potassium channels in dopamine transporter-mediated 6-hydroxydopamine neurotoxicity." Neuroscience **143**(1): 1-6.
Riederer, P. and S. Wuketich (1976). "Time course of nigrostriatal degeneration in parkinson's disease. A detailed study of influential factors in human brain amine analysis." J Neural Transm **38**(3-4): 277-301.
Ries, V., R. M. Silva, et al. (2008). "JNK2 and JNK3 combined are essential for apoptosis in dopamine neurons of the substantia nigra, but are not required for axon degeneration." J Neurochem **107**(6): 1578-1588.
Rodriguez-Oroz, M. C., J. A. Obeso, et al. (2005). "Bilateral deep brain stimulation in Parkinson's disease: a multicentre study with 4 years follow-up." Brain **128**(Pt 10): 2240-2249.
Rohe, C. F., P. Montagna, et al. (2004). "Homozygous PINK1 C-terminus mutation causing early-onset parkinsonism." Ann Neurol **56**(3): 427-431.
Saha, A. R., J. Hill, et al. (2004). "Parkinson's disease alpha-synuclein mutations exhibit defective axonal transport in cultured neurons." J Cell Sci **117**(Pt 7): 1017-1024.

Saito, Y., K. Nishio, et al. (2007). "Molecular mechanisms of 6-hydroxydopamine-induced cytotoxicity in PC12 cells: involvement of hydrogen peroxide-dependent and -independent action." Free Radic Biol Med **42**(5): 675-685.
Scatton, B., T. Dennis, et al. (1986). "Degeneration of noradrenergic and serotonergic but not dopaminergic neurones in the lumbar spinal cord of parkinsonian patients." Brain Res **380**(1): 181-185.
Schapira, A. H., J. M. Cooper, et al. (1990). "Mitochondrial complex I deficiency in Parkinson's disease." J Neurochem **54**(3): 823-827.
Schober, A. (2004). "Classic toxin-induced animal models of Parkinson's disease: 6-OHDA and MPTP." Cell Tissue Res **318**(1): 215-224.
Schrag, A. and J. M. Schott (2006). "Epidemiological, clinical, and genetic characteristics of early-onset parkinsonism." Lancet Neurol **5**(4): 355-363.
Shi, M., D. Majumdar, et al. (2013). "Glia co-culture with neurons in microfluidic platforms promotes the formation and stabilization of synaptic contacts." Lab Chip **13**(15): 3008-3021.
Shi, P., S. Nedelec, et al. (2010). "Combined microfluidics/protein patterning platform for pharmacological interrogation of axon pathfinding." Lab on a Chip **10**(8): 1005-1010.
Shi, W., H. Wen, et al. (2010). "Droplet microfluidics for characterizing the neurotoxin-induced responses in individual Caenorhabditis elegans." Lab Chip **10**(21): 2855-2863.
Shulman, J. M., P. L. De Jager, et al. (2011). "Parkinson's disease: genetics and pathogenesis." Annu Rev Pathol **6**: 193-222.
Singleton, A. B., M. Farrer, et al. (2003). "alpha-Synuclein locus triplication causes Parkinson's disease." Science **302**(5646): 841.
Spillantini, M. G., M. L. Schmidt, et al. (1997). "Alpha-synuclein in Lewy bodies." Nature **388**(6645): 839-840.
Staal, R. G. and P. K. Sonsalla (2000). "Inhibition of brain vesicular monoamine transporter (VMAT2) enhances 1-methyl-4-phenylpyridinium neurotoxicity in vivo in rat striata." J Pharmacol Exp Ther **293**(2): 336-342.
Surmeier, D. J., J. N. Guzman, et al. (2010). "What causes the death of dopaminergic neurons in Parkinson's disease?" Prog Brain Res **183**: 59-77.
Takeuchi, A., S. Nakafutami, et al. (2011). "Device for co-culture of sympathetic neurons and cardiomyocytes using microfabrication." Lab on a Chip **11**(13): 2268-2275.
Tanaka, A., M. M. Cleland, et al. (2010). "Proteasome and p97 mediate mitophagy and degradation of mitofusins induced by Parkin." J Cell Biol **191**(7): 1367-1380.
Tanida, I. (2011). "Autophagy basics." Microbiol Immunol **55**(1): 1-11.
Taylor, A. M., M. Blurton-Jones, et al. (2005). "A microfluidic culture platform for CNS axonal injury, regeneration and transport." Nat Methods **2**(8): 599-605.
Taylor, A. M., D. C. Dieterich, et al. (2010). "Microfluidic local perfusion chambers for the visualization and manipulation of synapses." Neuron **66**(1): 57-68.
Taylor, A. M., S. W. Rhee, et al. (2006). "Microfluidic chambers for cell migration and neuroscience research." Methods Mol Biol **321**: 167-177.
Taylor, A. M., S. W. Rhee, et al. (2003). "Microfluidic Multicompartment Device for Neuroscience Research." Langmuir **19**(5): 1551-1556.
Ungerstedt, U. (1968). "6-Hydroxy-dopamine induced degeneration of central monoamine neurons." Eur J Pharmacol **5**(1): 107-110.
Volpicelli-Daley, L. A., K. C. Luk, et al. (2011). "Exogenous alpha-synuclein fibrils induce Lewy body pathology leading to synaptic dysfunction and neuron death." Neuron **72**(1): 57-71.
Wakabayashi, K., H. Takahashi, et al. (1988). "Parkinson's disease: the presence of Lewy bodies in Auerbach's and Meissner's plexuses." Acta Neuropathol **76**(3): 217-221.

Wang, D., L. Qian, et al. (2006). "Antioxidants protect PINK1-dependent dopaminergic neurons in Drosophila." Proc Natl Acad Sci U S A **103**(36): 13520-13525.
Wang, H. L., A. H. Chou, et al. (2011). "PARK6 PINK1 mutants are defective in maintaining mitochondrial membrane potential and inhibiting ROS formation of substantia nigra dopaminergic neurons." Biochim Biophys Acta **1812**(6): 674-684.
Wang, J. T., Z. A. Medress, et al. (2012). "Axon degeneration: molecular mechanisms of a self-destruction pathway." J Cell Biol **196**(1): 7-18.
Wang, M., Y. Wu, et al. (2001). "The gene for slow Wallerian degeneration (Wld(s)) is also protective against vincristine neuropathy." Neurobiol Dis **8**(1): 155-161.
Wang, X., D. Winter, et al. (2011). "PINK1 and Parkin target Miro for phosphorylation and degradation to arrest mitochondrial motility." Cell **147**(4): 893-906.
Whitesides, G. M., E. Ostuni, et al. (2001). "Soft lithography in biology and biochemistry." Annu Rev Biomed Eng **3**: 335-373.
Wong, E. and A. M. Cuervo (2010). "Autophagy gone awry in neurodegenerative diseases." Nat Neurosci **13**(7): 805-811.
Xia, Y., E. Kim, et al. (1996). "Complex Optical Surfaces Formed by Replica Molding Against Elastomeric Masters." Science **273**(5273): 347-349.
Xia, Y. and G. M. Whitesides (1998). "SOFT LITHOGRAPHY." Annual Review of Materials Science **28**(1): 153-184.
Yang, Y., S. Gehrke, et al. (2006). "Mitochondrial pathology and muscle and dopaminergic neuron degeneration caused by inactivation of Drosophila Pink1 is rescued by Parkin." Proc Natl Acad Sci U S A **103**(28): 10793-10798.
Youle, R. J. and A. M. van der Bliek (2012). "Mitochondrial fission, fusion, and stress." Science **337**(6098): 1062-1065.
Yu, W., Y. Sun, et al. (2011). "The PINK1/Parkin pathway regulates mitochondrial dynamics and function in mammalian hippocampal and dopaminergic neurons." Hum Mol Genet **20**(16): 3227-3240.
Zhao, X.-M., Y. Xia, et al. (1997). "Soft lithographic methods for nano-fabrication." Journal of Materials Chemistry **7**(7): 1069-1074.
Zimprich, A., S. Biskup, et al. (2004). "Mutations in LRRK2 cause autosomal-dominant parkinsonism with pleomorphic pathology." Neuron **44**(4): 601-607.